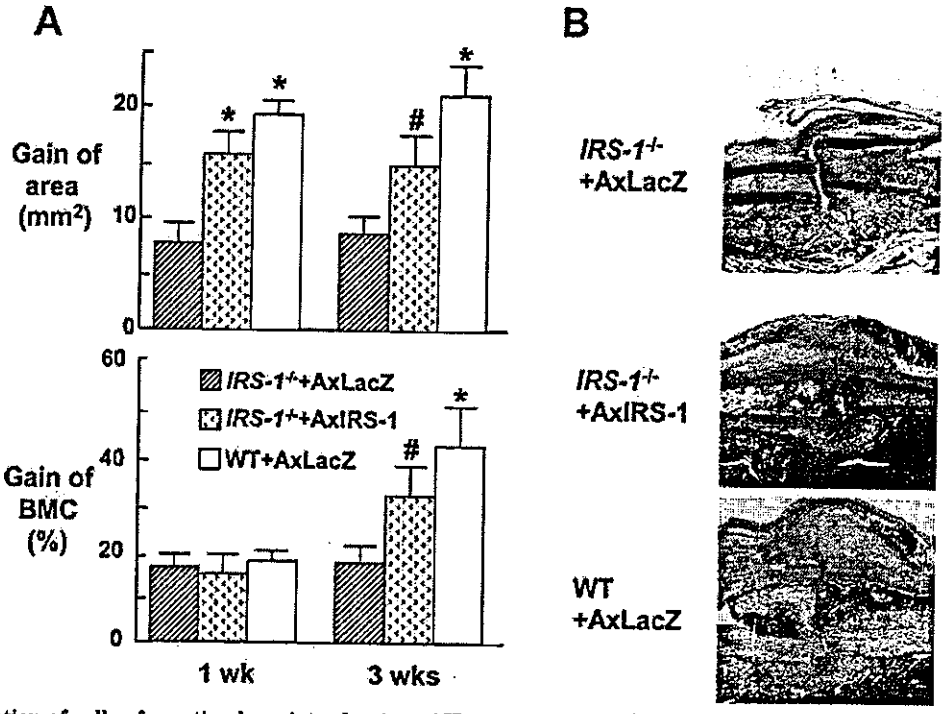

FIG. 5. **Restoration of callus formation by reintroduction of IRS-1 in the *IRS-1*$^{-/-}$ fracture using an adenovirus vector carrying *IRS-1* gene (AxIRS1) or *lacZ* (AxLacZ).** *A*, the gain of area (*upper panel*) and the % gain of BMC (*lower panel*) of the callus in AxLacZ- or AxIRS1-injected *IRS-1*$^{-/-}$ mice and AxLacZ-injected WT mice. AxIRS-1 or AxLacZ was injected into the fracture site of *IRS-1*$^{-/-}$ or WT mice 2 days after the fracture, and animals were sacrificed at 1 week and 3 weeks after the injection. The parameters during the observation periods as compared with those at time 0 were calculated for the entire tibiae of fractured and unfractured sides, and the differences were compared between WT and *IRS-1*$^{-/-}$. Data are expressed as the mean (*bars*) ± S.E. (*error bars*) for 3 mice/group. #, $p < 0.05$; *, $p < 0.01$ *versus* *IRS-1*$^{-/-}$+AxLacZ. *B*, HE staining of the callus 1 week after the injection.

ther the cellular mechanisms underlying these abnormalities, we used our original method to isolate chondrocytes from the growth plate. We first confirmed the purity of the growth plate chondrocytes by the X-gal staining of cultured chondrocytes isolated by this method from the transgenic mice expressing the *lacZ* reporter gene driven by a promoter fragment of type I collagen (*COL1-LacZ*) or type II collagen gene (*COL2-LacZ*) (26, 27). More than 99% of the cells isolated from transgenic mice with the type II collagen promoter were stained X-gal-positive, indicating positive *lacZ* transgene expression, whereas none of the cells from type I collagen promoter-driving transgenic mice exhibited the expression (Fig. 6*A*). These results demonstrate that almost all cells isolated from the growth plate by this method are cells of chondrocyte lineage and are not contaminated by other cells such as osteoblasts or fibroblasts, which express type I collagen.

To confirm the expression patterns of IRS-1 and IRS-2 as shown in Fig. 3*A*, we examined the protein levels in the growth plate chondrocytes by Western blottings using the same antibodies as Fig. 3*A* (Fig. 6*B*). WT chondrocytes, but not *IRS-1*$^{-/-}$ chondrocytes, were shown to express the IRS-1 protein; however, neither WT nor *IRS-1*$^{-/-}$ chondrocytes expressed IRS-2. This was not due to the lack of immunoreactivity of the IRS-2 antibody since IRS-2 protein could be detected in primary osteoblasts, the positive control cells that we studied previously (20).

We then compared DNA synthesis and proliferation of the primary chondrocytes between WT and *IRS-1*$^{-/-}$ by the [^{3}H]TdR uptake (Fig. 6*C*) and the growth curve (Fig. 6*D*), respectively. *IRS-1*$^{-/-}$ chondrocytes showed significantly reduced [^{3}H]TdR uptake as compared with WT chondrocytes in the control culture (Fig. 6*C*). Both IGF-I and insulin significantly stimulated the DNA synthesis of WT chondrocytes but not that of *IRS-1*$^{-/-}$ chondrocytes. On the other hand, the stimulation by FGF-2 was similarly seen in both WT and *IRS-1*$^{-/-}$ chondrocytes, indicating that impaired DNA synthesis in cultured *IRS-1*$^{-/-}$ chondrocytes was specific to IGF-I and insulin. The growth curve for 9 days after the seeding confirmed the impaired mitogenic ability of *IRS-1*$^{-/-}$ chondrocytes (Fig. 6*D*). The number of these chondrocytes was significantly lower than that of WT chondrocytes at 7 days and thereafter in the control cultures, and the difference was enhanced in the presence of IGF-I.

Signal Transduction in Cultured Primary Chondrocytes—To provide some insight into signaling pathways that are affected by the IRS-1 deficiency in chondrocytes, we compared the activation of PI3K/Akt and MAPKs, the main signals lying downstream of IRS-1, between WT and *IRS-1*$^{-/-}$ growth plate chondrocytes (Fig. 7*A*). Western blot analyses of the WT chondrocytes revealed that IGF-I induced phosphorylations of Akt and ERK but not that of p38 MAPK. Specific inhibitors, LY294002, PD98059, and SB203580, were confirmed to inhibit the phosphorylations of Akt, ERK, and p38 MAPK, respectively. In the *IRS-1*$^{-/-}$ chondrocytes, the Akt phosphorylation by IGF-I was reduced as compared with that of WT chondrocytes; however, phosphorylations of ERK and p38 MAPK were similar between WT and *IRS-1*$^{-/-}$ chondrocytes. The decrease in the Akt phosphorylation by the IRS-1 deficiency was confirmed by quantitative analyses using densitometry in independent Western blottings of three separate experiments (Fig. 7*B*). These results indicate that the IRS-1 deficiency led to impairment of the PI3K/Akt pathway but not the MAPK pathways.

To examine further the involvement of these signaling pathways in the mitogenic action of IGF-I on the WT and *IRS-1*$^{-/-}$ chondrocytes, the inhibitors above were added to the chondro-

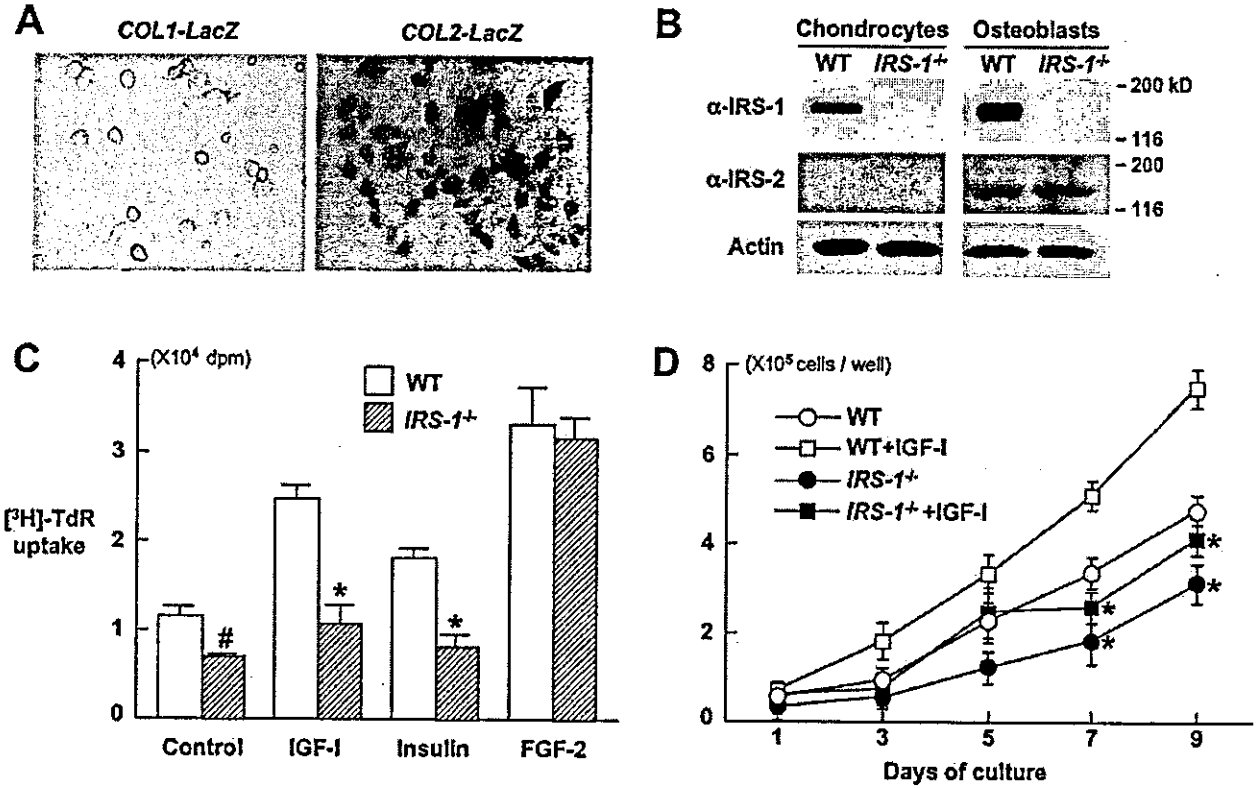

FIG. 6. **Characterization and proliferation of chondrocytes isolated from WT and *IRS-1*$^{-/-}$ growth plates.** *A*, chondrocytes were isolated from epiphyseal growth plates of WT and *IRS-1*$^{-/-}$ mice at 3.5 weeks of age as described under "Experimental Procedures." To confirm the purity of chondrocytes, cells were isolated from the growth plates of transgenic mice expressing the *lacZ* reporter gene driven by the type I collagen promoter gene fragment (*COL1-LacZ*) or the type II collagen promoter gene fragment (*COL2-LacZ*). LacZ activity was visualized as *blue* with X-gal staining. *B*, Western blottings for the IRS-1 and IRS-2 expressions in the growth plate chondrocytes and calvarial osteoblasts derived from WT and *IRS-1*$^{-/-}$ mice. Antibodies for IRS-1 and IRS-2 (α-IRS-1 and α-IRS-2) were the same as those used in the immunohistochemical analyses (Fig. 3*A*). *C*, DNA synthesis determined by [^{3}H]TdR uptake in chondrocytes isolated from WT and *IRS-1*$^{-/-}$ growth plates cultured with and without insulin (100 nM), IGF-I (10 nM), or FGF-2 (10 nM) for 18 h. Data are expressed as the mean (*bars*) ± S.E. (*error bars*) for 8 wells/group. #, $p < 0.05$; *, $p < 0.01$ *versus* WT culture. *D*, cell proliferation determined by growth curves of chondrocytes that were isolated from WT and *IRS-1*$^{-/-}$ growth plates and cultured in the presence and absence of IGF-I. Chondrocytes were inoculated at a density of 10^5 cells/well in 6-multiwell plates, and the number of the cells/well was counted 1, 3, 5, 7, and 9 days after the seeding. Data are expressed as the mean (*symbols*) ± S.E. (*error bars*) for 6 wells/group. *, $p < 0.01$; significant decrease by the IRS-1 deficiency.

cyte cultures (Fig. 7*C*). LY294002, an Akt inhibitor, dose-dependently decreased the stimulation of [^{3}H]TdR uptake by IGF-I in the WT culture; however, in the *IRS-1*$^{-/-}$ culture, the inhibition was not statistically significant ($p > 0.05$). PD98059, an ERK inhibitor, decreased the IGF-I mitogenic effect at the highest concentration of 10 μM both in the WT and *IRS-1*$^{-/-}$ cultures ($p < 0.01$), whereas SB203580, a p38 inhibitor, did not affect it in either culture. Taken together, these results suggest that the mitogenic action of IGF-I is mediated largely by the IRS-1-dependent pathway through the PI3K/Akt activation and partly by IRS-1-independent pathway through the ERK activation.

DISCUSSION

Although IRS-1 and IRS-2 are known to be essential for intracellular signaling of IGF-I/insulin, these two adaptor molecules have distinct biological roles and are differentially expressed in a variety of cells. Regarding glucose homeostasis, IRS-1 plays an important role in the metabolic actions of insulin mainly in skeletal muscle and adipose tissue, whereas IRS-2 does so in the liver (29, 30). For bone metabolism, although both are expressed in osteoblasts, they play distinct roles in the anabolic function of IGF-I and insulin (19, 20). The present study, however, failed to detect the IRS-2 expression in isolated chondrocytes or fracture callus. Our previous studies also revealed that IRS-2 was not expressed in the epiphyseal cartilage (31) and that *IRS-2*$^{-/-}$ mice showed normal epiphyseal cartilage and skeletal growth as opposed to *IRS-1*$^{-/-}$ mice (20). We therefore speculate that IRS-2 is much less important than IRS-1 in bone regeneration through endochondral ossification such as bone healing and skeletal growth. In fact, our preliminary experiment showed no abnormality of bone healing in *IRS-2*$^{-/-}$ mice (data not shown).

Because histological examinations suggested the central role of abnormal chondrocyte functions in the impairment of bone healing by the IRS-1 deficiency, we focused on the chondrocyte culture to study the cellular and molecular mechanisms. For this study, we avoided using the conventional chondrocyte culture system derived from the rib cartilage of neonatal mice (32), because most of the cartilage belongs to the permanent cartilage that does not undergo endochondral ossification but maintains cartilage phenotypes. Instead, we succeeded in isolating chondrocytes from the growth plate with more than 99% purity, as confirmed by the X-gal staining of cultured cells from transgenic mice expressing osteoblast- or chondrocyte-specific marker genes (Fig. 6*A*). Our preliminary study has confirmed that the growth plate chondrocytes showed much higher ability of proliferation than the rib chondrocytes. However, neither hypertrophic differentiation nor apoptosis could be clearly observed even after long term culture of the growth plate chondrocytes. Hence, although we believe that the present chon-

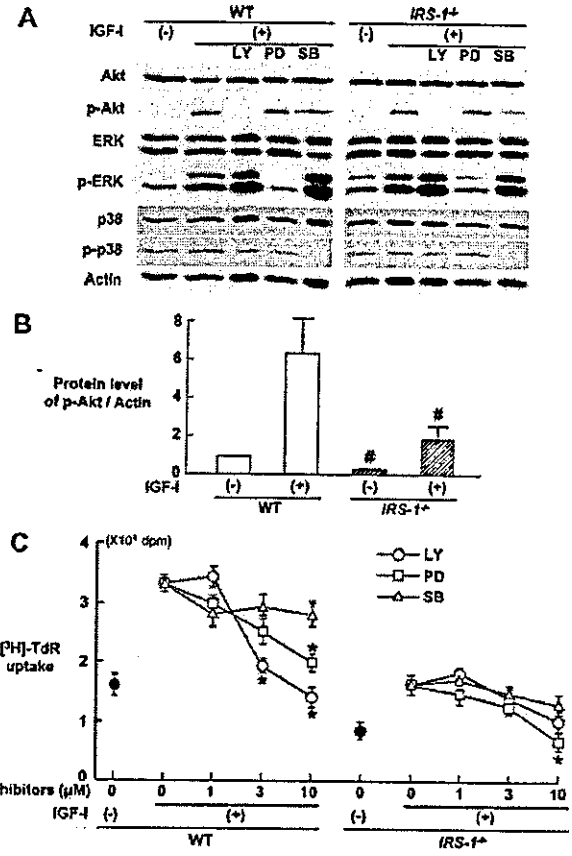

FIG. 7. **Intracellular signaling in the WT and *IRS-1*$^{-/-}$ growth plate chondrocytes.** *A*, effects of IGF-1 and specific inhibitors on phosphorylations of Akt, ERK, and p38 MAPK in cultured chondrocytes. The chondrocytes were isolated as above and cultured with and without IGF-I (10 nM) in the presence and absence of an Akt inhibitor LY294002 (*LY*, 10 μM), an ERK inhibitor PD98059 (*PD*, 10 μM), and p38 MAPK inhibitor SB203580 (*SB*, 10 μM) for 30 min. Western blottings were performed as described under "Experimental Procedures." *B*, quantitative analysis of phospho-Akt (*p-Akt*) levels determined by three independent Western blottings using samples from separate experiments including that above (*A*). The *ordinate axis* shows the intensity of the p-Akt band normalized to that of β-actin measured by densitometry. The graph indicates means (*bars*) ± S.E. (*error bars*) of the ratio values as compared with that of WT control group in three independent experiments. #, $p < 0.05$; significant decrease by the IRS-1 deficiency. *C*, effects of specific inhibitors on the mitogenic action of IGF-I in cultured primary chondrocytes. The primary chondrocytes were cultured with and without IGF-I (10 nM), LY294002 (1, 3, and 10 μM), PD98059 (1, 3, and 10 μM), and SB203580 (1, 3, and 10 μM). After 18 h of culture, DNA synthesis was determined by [^{3}H]TdR uptake. Data are expressed as means (*symbols*) ± S.E. (*error bars*) for 8 wells/group. *, $p < 0.01$, significant inhibition by LY294002, PD98059, or SB203580.

drocyte culture system is more suitable for studies on the proliferation of chondrocytes than the conventional culture system, a culture system of primary cells isolated directly from the fracture callus will be much more appropriate to study the mechanisms underlying impaired fracture healing in *IRS-1*$^{-/-}$ mice. In fact, we initially tried to use these callus-derived cells for the culture; however, the callus was composed of cells of heterogeneous kinds at various differentiation stages so that the data were too inconsistent to compare among animals.

The *IRS-1*$^{-/-}$ callus exhibited not only a decrease in proliferation of chondrocytes but also increases in hypertrophic differentiation and apoptosis (Fig. 4). This is compatible with our histological findings of the *IRS-1*$^{-/-}$ growth plate, which showed a decrease in the height of the proliferating zone and an early closure of the growth plate, resulting in a reduced longitudinal bone growth (31). Although the mechanism of the decrease in chondrocyte proliferation by the IRS-1 deficiency was shown by the growth plate chondrocyte cultures, that of the increase in differentiation or apoptosis remains unclarified. Because chondrocytes are known to start hypertrophic differentiation in synchrony with the cessation of proliferation, the acceleration of chondrocyte differentiation and the subsequent apoptosis seen in the *IRS-1*$^{-/-}$ fracture callus and growth plate might be secondary to the impairment of proliferation. However, there are several reports (33–38) showing that IRS-1 directly inhibits differentiation and apoptosis in hemopoietic and neuronal cells and that these inhibitions are partly associated with an increase in the cell size. Although the present *in vivo* and *in vitro* studies did not find the change of cell size of chondrocytes by the IRS-1 deficiency, the possible involvement of direct action of IRS-1 signaling in differentiation and apoptosis cannot be denied. As mentioned above, studies on these aspects using a culture system of other primary chondrocytes in which both hypertrophy and apoptosis can be properly assessed will be the next task for investigation.

The decreased [^{3}H]TdR uptake in *IRS-1*$^{-/-}$ chondrocytes was seen not only in the stimulated culture by IGF-I or insulin but also in the control culture (Fig. 6*C*). This may be due to the blockage of signalings of endogenous IGF-I as an autocrine/paracrine factor in the culture. The concentrations of IGF-I in the culture medium were 0.79 ± 0.20 and 0.66 ± 0.15 nM (mean ± S.E.) in the control WT and *IRS-1*$^{-/-}$ cultures, respectively. In addition, our previous study has shown that serum IGF-I levels were similar between WT and *IRS-1*$^{-/-}$ mice, suggesting the absence of systemic compensation for impaired IGF-I activity (19). Hence, the impaired fracture healing in *IRS-1*$^{-/-}$ mice might be due to the deficit of anabolic signaling of endogenous IGF-I produced by chondrocytes acting as an autocrine/paracrine factor. Impairment of *IRS-1*$^{-/-}$ fracture healing might partly be caused by systemic hormones, of which actions are mediated by IGF-I. Growth hormone is a well known stimulus of IGF-I production in a variety of tissues, including bone, and exerts its effects on bone mainly through IGF-I mediation (39). Parathyroid hormone also increases IGF-I production, and decreases of IGF-I signaling can block selective anabolic actions of parathyroid hormone on bone (40, 41). Similarly, other hormones with effects on bone such as cortisol (42), thyroid hormone (43), estrogen (44), and androgens (45) alter IGF-I levels in bone in a manner consistent with IGF-I playing a role in the actions of these hormones on bone.

It is noteworthy that skeletal phenotypes of IGF-I receptor (IGF-IR) and IGF-I-deficient mice are rather different from that of *IRS-1*$^{-/-}$ mice. First, they exhibit more severe growth retardation than do *IRS-1*$^{-/-}$ mice (5, 6, 46). More important, the closure of the growth plate is delayed in *IGF-I*$^{-/-}$ mice (5, 6), whereas it is accelerated in *IRS-1*$^{-/-}$ mice (31). These discrepancies might be due to the 66-kDa Src homology collagen (SHC), another adaptor protein phosphorylated by the IGF-IR activation, which is reported to be expressed in chondrocytes and osteoblasts (47, 48). SHC is known to associate with growth factor receptor-bound protein 2, p21 Ras, and a serine/threonine kinase cascade leading to the activation of ERK in chondrocytes (47, 49, 50). Our Western blotting data that IGF-I induced phosphorylations of both Akt and ERK, whereas IRS-I deficiency decreased only the Akt phosphorylation in Fig. 7*A*, support the existence of SHC/ERK pathway in chondrocytes. Inhibition of this pathway by PD98059 may cause the suppression of the IGF-I mitogenic effect in both WT and *IRS-1*$^{-/-}$

cultures (Fig. 7*C*). Most interesting, IGF-I induced the Akt phosphorylation not only in WT but also in *IRS-1*$^{-/-}$ chondrocytes (Fig. 7, *A* and *B*), suggesting the involvement of SHC/Ark pathway in a downstream signaling of IGF-IR activation. This pathway, however, seems functionally less important than IRS-1/Akt and SHC/ERK pathways, because the inhibition by LY294002 was not statistically significant in the *IRS-1*$^{-/-}$ culture (Fig. 7*C*). It is also important that the SHC signaling positively regulates apoptosis (51). A decrease in the apoptotic pathway through SHC may cause the delay of the growth plate closure in the *IGF-I*$^{-/-}$ mice, whereas the compensatory up-regulation of the SHC signaling might lead to accelerated apoptosis of chondrocytes at the fracture callus and the growth plate in *IRS-1*$^{-/-}$ mice. Studies on the skeletal phenotype of the SHC-deficient mice will lead to elucidation of the differential regulation of bone regeneration by IRS-1 and SHC signalings.

We hereby conclude that the IRS-1 deficiency impairs bone healing at least partly by inhibiting the chondrocyte proliferation through the PI3K/Akt pathway, and we propose that IRS-1 can be a target molecule for bone regenerative medicine. There are several recent reports (52, 53) that used bone fracture models to identify *in vivo* signalings, such as tumor necrosis factor-α and cyclooxygenase-2, which play essential roles in the osteogenic process. Because IRS-1 is an intracellular protein, we are planning to use the gene transfer into precursor cells by using conventional natural viruses or nonviral vectors that we are now developing (54). In the present study, the *in vivo* fracture system and the *in vitro* chondrocyte culture system were applied for the first time in combination to investigate the role of a certain molecule in knockout mice. This approach seems useful for elucidating a network of molecules implicated in bone regeneration.

REFERENCES

1. Bolander, M. E. (1992) *Proc. Soc. Exp. Biol. Med.* **200**, 165–170
2. Kawaguchi, H., Kurokawa, T., Hanada, K., Hiyama, Y., Tamura, M., Ogata, E., and Matsumoto, T. (1994) *Endocrinology* **135**, 774–781
3. Canalis, E. (1993) *Bone (NY)* **14**, 273–276
4. Laron, Z. (2001) *Mol. Pathol.* **54**, 311–316
5. Liu, J. P., Baker, J., Perkins, A. S., Robertson, E. J., and Efstratiadis, A. (1993) *Cell* **75**, 59–72
6. Powell-Braxton, L., Hollingshead, L. P., Warburton, C., Dowd, M., Pitts-Meek, S., Dalton, D., Gillett, N., and Stewart, T. A. (1993) *Genes Dev.* **7**, 2609–2617
7. Laron, Z., Klinger, B., and Silbergeld, A. (1999) *J. Bone Miner. Res.* **14**, 156–157
8. Trippel, S. B. (1998) *Clin. Orthop. Relat. Res.* **355**, S301–S313
9. Schmidmaier, G., Wildemann, B., Heeger, J., Gabelein, T., Flyvbjerg, A., Bail, H. J., and Raschke, M. (2002) *Bone (NY)* **31**, 165–172
10. Thomas, D. M., Hards, D. K., Rogers, S. D., Ng, K. W., and Best, J. D. (1997) *Endocrinol. Metab. Clin North Am.* **4**, 5–17
11. Shukunami, C., Shigeno, C., Atsumi, T., Ishizeki, K., Suzuki, F., and Hiraki, Y. (1996) *J. Cell Biol.* **133**, 457–468
12. Kato, Y., and Gospodarowicz, D. (1984) *J. Cell Physiol.* **120**, 354–363
13. Krakauer, J. C., McKenna, M. J., Rao, D. S., and Whitehouse, F. W. (1997) *Diabetes Care* **20**, 1339–1340
14. Piepkorn, B., Kann, P., Forst, T., Andreas, J., Pfutzner, A., and Beyer, J. (1997) *Horm. Metab. Res.* **29**, 584–591
15. Macey, L. R., Kana, S. M., Jingushi, S., Terek, R. M., Borretos, J., and Bolander, M. E. (1989) *J. Bone Jt. Surg. Am.* **71**, 722–733
16. Loder, R. T. (1988) *Clin. Orthop.* **232**, 210–216
17. Burks, D. J., and White, M. F. (2001) *Diabetes* **50**, Suppl. 1, 140–145
18. Kadowaki, T., Tobe, K., Honda-Yamamoto, R., Tamemoto, H., Kaburagi, Y., Momomura, K., Ueki, K., Takahashi, Y., Yamauchi, T., Akanuma, Y., and Yazaki, Y. (1996) *Endocr. J.* **43**, (suppl.) 33–41
19. Ogata, N., Chikazu, D., Kubota, N., Terauchi, Y., Tobe, K., Azuma, Y., Ohta, T., Kadowaki, T., Nakamura, K., and Kawaguchi, H. (2000) *J. Clin. Investig.* **105**, 935–943
20. Akune, T., Ogata, N., Hoshi, K., Kubota, N., Terauchi, Y., Tobe, K., Azuma, Y., Kadowaki, T., Nakamura, K., and Kawaguchi, H. (2002) *J. Cell Biol.* **159**, 147–156
21. Tamemoto, H., Kadowaki, T., Tobe, K., Yagi, T., Sakura, H., Hayakawa, T., Terauchi, Y., Ueki, K., Kaburagi, Y., Satoh, S., Sekihara, H., Yoshioka, Y., Horikoshi, H., Furuta, Y., Ikawa, Y., Kasuga, M., Yazaki, Y., and Aizawa, S. (1994) *Nature* **372**, 182–186
22. Kubota, N., Tobe, K., Terauchi, Y., Eto, K., Yamauchi, T., Suzuki, R., Tsubamoto, Y., Komeda, K., Nakano, R., Miki, H., Satoh, S., Sekihara, H., Sciacchitano, S., Lesniak, M., Aizawa, S., Nagai, R., Kimura, S., Akanuma, Y., Taylor, S. I., and Kadowaki, T. (2000) *Diabetes* **49**, 1880–1889
23. Smink, J. J., Gresnigt, M. G., Hamers, N., Koedam, J. A., Berger, R., and Van Buul-Offers, S. C. (2003) *J. Endocrinol.* **177**, 381–388
24. van Griensven, M., Lobenhoffer, P., Barke, A., Tschernig, T., Lindenmaier, W., Krettek, C., and Gerich, T. G. (2002) *Lab. Anim.* **36**, 455–461
25. Uusitalo, H., Hiltunen, A., Ahonen, M., Gao, T. J., Lefebvre, V., Harley, V., Kahari, V. M., and Vuorio, E. (2001) *J. Bone Miner. Res.* **16**, 1837–1845
26. Liu, W., Toyosawa, S., Furuichi, T., Kanatani, N., Yoshida, C., Liu, Y., Himeno, M., Narai, S., Yamaguchi, A., and Komori, T. (2001) *J. Cell Biol.* **155**, 157–166
27. Ueta, C., Iwamoto, M., Kanatani, N., Yoshida, C., Liu, Y., Enomoto-Iwamoto, M., Ohmori, T., Enomoto, H., Nakata, K., Takada, K., Kurisu, K., and Komori, T. (2001) *J. Cell Biol.* **153**, 87–100
28. Shimoaka, T., Ogasawara, T., Yonamine, A., Chikazu, D., Kawano, H., Nakamura, K., Itoh, N., and Kawaguchi, H. (2002) *J. Biol. Chem.* **277**, 7493–7500
29. Bruning, J. C., Winnay, J., Cheatham, B., and Kahn, C. R. (1997) *Mol. Cell. Biol.* **17**, 1513–1521
30. Yamauchi, T., Tobe, K., Tamemoto, H., Ueki, K., Kaburagi, Y., Yamamoto-Honda, R., Takahashi, Y., Yoshizawa, F., Aizawa, S., Akanuma, Y., Sonenberg, N., Yazaki, Y., and Kadowaki, T. (1996) *Mol. Cell. Biol.* **16**, 3074–3084
31. Hoshi, K., Ogata, N., Shimoaka, T., Terauchi, Y., Kadowaki, T., Kenmotsu, S., Chung, U., Ozawa, H., Nakamura, K., and Kawaguchi, H. (2004) *J. Bone Miner. Res.* **19**, 214–223
32. Lefebvre, V., Garofalo, S., Zhou, G., Mesaranta, M., Vuorio, E., and de Crombrugghe, B. (1994) *Matrix Biol.* **14**, 329–335
33. Valentinis, B., and Baserga, R. (2001) *Mol. Pathol.* **54**, 133–137
34. Morrione, A., Navarro, M., Romano, G., Dews, M., Reiss, K., Valentinis, B., Belletti, B., and Baserga, R. (2001) *Oncogene* **20**, 4842–4852
35. Valentinis, B., Navarro, M., Zanocco-Marani, T., Edmonds, P., McCormick, J., Morrione, A., Sacchi, A., Romano, G., Reiss, K., and Baserga, R. (2000) *J. Biol. Chem.* **275**, 25451–25459
36. Peruzzi, F., Prisco, M., Dews, M., Salomoni, P., Grassilli, E., Romano, G., Calabretta, B., and Baserga, R. (1999) *Mol. Cell. Biol.* **19**, 7203–7215
37. Hermanto, U., Zong, C. S., Li, W., and Wang, L. H. (2002) *Mol. Cell. Biol.* **22**, 2345–2365
38. Pende, M., Kozma, S. C., Jaquet, M., Oorschot, V., Burcelin, R., Le Marchand-Brustel, Y., Klumperman, J., Thorens, B., and Thomas, G. (2000) *Nature* **408**, 994–997
39. Ohlsson, C., Bengtsson, B. A., Isaksson, O. G., Andreassen, T. T., and Slootweg, M. C. (1998) *Endocr. Rev.* **19**, 55–79
40. Canalis, E., Centrella, M., Burch, W., and McCarthy, T. L. (1989) *J. Clin. Investig.* **83**, 60–65
41. Miyakoshi, N., Kasukawa, Y., Linkhart, T. A., Baylink, D. J., and Mohan, S. (2001) *Endocrinology* **142**, 4349–4356
42. McCarthy, T. L., Centrella, M., and Canalis, E. (1990) *Endocrinology* **126**, 1569–1575
43. Huang, B. K., Golden, L. A., Tarjan, G., Madison, L. D., and Stern, P. H. (2000) *J. Bone Miner. Res.* **15**, 188–197
44. Ernst, M., and Rodan, G. A. (1991) *Mol. Endocrinol.* **5**, 1081–1089
45. Gori, F., Hofbauer, L. C., Conover, C. A., and Khosla, S. (1999) *Endocrinology* **140**, 5579–5586
46. Araki, E., Lipes, M. A., Patti, M. E., Bruning, J. C., Haag, B., Johnson, R. S., and Kahn, C. R. (1994) *Nature* **372**, 186–190
47. Shakibaei, M., John, T., De Souza, P., Rahmanzadeh, R., and Merker, H. J. (1999) *Biochem. J.* **342**, 615–623
48. Caverzasio, J., Palmer, G., Suzuki, A., and Bonjour, J. P. (1997) *J. Bone Miner. Res.* **12**, 1975–1983
49. Lopaczynski, W. (1999) *Acta Biochim. Pol.* **46**, 51–60
50. Benito, M., Valverde, A. M., and Lorenzo, M. (1996) *Int. J. Biochem. Cell Biol.* **28**, 499–510
51. Migliaccio, E., Giorgio, M., Mele, S., Pelicci, G., Reboldi, P., Pandolfi, P. P., Lanfrancone, L., and Pelicci, P. G. (1999) *Nature* **402**, 309–313
52. Zhang, X., Schwarz, E. M., Young, D. A., Puzas, J. E., Rosier, R. N., and O'Keefe, R. J. (2002) *J. Clin. Investig.* **109**, 1405–1415
53. Gerstenfeld, L. C., Cho, T. J., Kon, T., Aizawa, T., Tsay, A., Fitch, J., Barnes, G. L., Graves, D. T., and Einhorn, T. A. (2003) *J. Bone Miner. Res.* **18**, 1584–1592
54. Itaka, K., Harada, A., Nakamura, K., Kawaguchi, H., and Kataoka, K. (2002) *Biomacromolecules* **3**, 841–845

JOURNAL OF BONE AND MINERAL RESEARCH
Volume 19, Number 7, 2004
Published online on May 24, 2004; doi: 10.1359/JBMR.040513

Osteoclast Differentiation by RANKL Requires NF-κB–Mediated Downregulation of Cyclin-Dependent Kinase 6 (Cdk6)

Toru Ogasawara,[1] Mika Katagiri,[1] Aiichiro Yamamoto,[1] Kazuto Hoshi,[1] Tsuyoshi Takato,[1] Kozo Nakamura,[1] Sakae Tanaka,[1] Hiroto Okayama,[2] and Hiroshi Kawaguchi[1]

ABSTRACT: This study investigated the involvement of cell cycle factors in RANKL-induced osteoclast differentiation. Among the G1 cell cycle factors, Cdk6 was found to be a key molecule in determining the differentiation rate of osteoclasts as a downstream effector of the NF-κB signaling.

Introduction: A temporal arrest in the G1 phase of the cell cycle is a prerequisite for cell differentiation, making it possible that cell cycle factors regulate not only the proliferation but also the differentiation of cells. This study investigated cell cycle factors that critically influence differentiation of the murine monocytic RAW264.7 cells to osteoclasts induced by RANKL.

Materials and Methods: Growth-arrested RAW cells were stimulated with serum in the presence or absence of soluble RANKL (100 ng/ml). Expressions of the G1 cell cycle factors cyclin D1, D2, D3, E, cyclin-dependent kinase (Cdk) 2, 4, 6, and Cdk inhibitors (p18 and p27) were determined by Western blot analysis. Involvement of NF-κB and c-*jun* N-terminal kinase (JNK) pathways was examined by overexpressing dominant negative mutants of the *IκB kinase 2* (IKK^{DN}) gene and *mitogen-activated protein kinase kinase 7* ($MKK7^{DN}$) gene, respectively, using the adenovirus vectors. To determine the direct effect of Cdk6 on osteoclast differentiation, stable clones of RAW cells transfected with *Cdk6* cDNA were established. Osteoclast differentiation was determined by TRACP staining, and cell cycle regulation was determined by BrdU uptake and flow cytometric analysis.

Results and Conclusion: Among the cell cycle factors examined, the Cdk6 level was downregulated by RANKL synchronously with the appearance of multinucleated osteoclasts. Inhibition of the NF-κB pathway by IKK^{DN} overexpression, but not that of the JNK pathway by $MKK7^{DN}$ overexpression, caused the decreases in both Cdk6 downregulation and osteoclastogenesis by RANKL. RAW cells overexpressing Cdk6 resist RANKL-induced osteoclastogenesis; however, cell cycle regulation was not affected by the levels of Cdk6 overexpression, suggesting that the inhibitory effect of Cdk6 on osteoclast differentiation was not exerted through cell cycle regulation. These results indicate that Cdk6 is a critical regulator of RANKL-induced osteoclast differentiation and that its NF-κB–mediated downregulation is essential for efficient osteoclast differentiation.

J Bone Miner Res 2004;19:1128–1136. Published online on May 24, 2004; doi: 10.1359/JBMR.040513

Key words: osteoclast, cyclin, cell cycle, RANKL, bone

INTRODUCTION

OSTEOCLASTS ARE DERIVED from hematopoietic myeloid precursors of monocyte/macrophage lineage under the control of systemic and local factors produced by supporting cells such as osteoblasts and bone marrow stromal cells. Among these factors, RANKL is a TNF-related cytokine that stimulates osteoclast differentiation from hematopoietic precursor cells both in vitro and in vivo.[1–3] Mice lacking in either RANKL or its receptor RANK have defects in osteoclast differentiation that lead to severe osteopetrosis.[4–6] RANK is expressed on the surface of osteoclast progenitor cells and induces intracellular signals, leading to osteoclastogenesis on ligand binding or agonistic anti-RANK antibody stimulation.[6,7] Like other TNF receptor superfamily members, RANK stimulation can induce NF-κB, probably through association with several TNF receptor–associated factors (TRAFs): TRAF2, TRAF5, and TRAF6.[6,8–11] Mice deficient in both p50 and p52 subunits of NF-κB have been found to be osteopetrotic because of the failure in osteoclast differentiation, indicating a crucial role of NF-κB in osteoclastogenesis.[12,13] NF-κB activation requires sequential phosphorylation, ubiquitination, and degradation of the inhibitory subunit IκB as well as consequent exposure of a nuclear localization signal on NF-κB.[14–16] IκB kinase (IKK) signalsome is the protein complex that contains the inducible IκB kinase activity and consists of IKK1 (IKKα), IKK2 (IKKβ), and the NF-κB essential modulator (NEMO

The authors have no conflict of interest.

[1]Department of Sensory and Motor System Medicine, The University of Tokyo Graduate School of Medicine, Tokyo, Japan; [2]Department of Biochemistry and Molecular Biology, The University of Tokyo Graduate School of Medicine, Tokyo, Japan.

or IKKγ). Among these three components of IKK signalsome, both IKK1 and IKK2 seem to play a critical role in IκB phosphorylation. However, the studies of IKK1 and IKK2 knockout mice indicate that IKK2 is more potent for NF-κB activation by proinflammatory stimuli than IKK1.[17–20] This evidence suggests that IKK2 may have a vital function in RANKL-induced NF-κB activation, and in fact, we previously reported that the dominant negative IKK2 ($IKK2^{DN}$) overexpression suppressed both NF-κB activity and osteoclast formation induced by RANKL using the murine monocytic RAW264.7 cell culture.[21]

Proliferation of eukaryotic cells depends on their progression through the cell cycle, and at least a temporal cell cycle arrest at the G1 phase is thought to be a prerequisite for cell differentiation.[22] Cell cycle control is achieved through the actions of a family of cyclins and cyclin-dependent protein kinases (Cdk's), which phosphorylate and thereby activate cell cycle factors essential for the onset of the next cell cycle phase. In mammalian cells, traverse through G1 and subsequent S phase entry require the activities of the cyclin D-dependent kinases Cdk4 and/or Cdk6 and the cyclin E-dependent kinase Cdk2. These Cdk's are negatively regulated by inhibitory proteins (CKIs) through direct binding to themselves.[23,24] CKIs have been classified into two families: INK4 and Cip/Kip. INK4 (p16, p15, p18, and p19) inhibits only Cdk4 and Cdk6, whereas Cip/Kip (p21, p27, and p57) inhibits all the Cdk's except for the Cdk6-cyclin D3 complex.[25] Because the control of cell cycle factors driving S phase onset greatly influences the commitment to cell differentiation in lower eukaryotes, this study investigated the possibility of crucial participation of some cell cycle start factors in RANKL-induced osteoclast differentiation and found that on RANKL treatment Cdk6 was downregulated primarily by RANKL/NF-κB signal-invoked transcriptional repression and that its downregulation was essential for efficient osteoclast differentiation.

MATERIALS AND METHODS

Reagents and antibodies

Human soluble recombinant RANKL was purchased from Wako Pure Chemicals (Osaka, Japan). Recombinant human macrophage-colony stimulating factor (M-CSF) was purchased from R&D Systems (Minneapolis, MN, USA). Antibodies against Cdk2 (H-298), Cdk4 (C-22), Cdk6 (C-21), cyclin D1 (C-20), cyclin D2 (M-20), cyclin D3 (C-16), cyclin E (M-20), p18 (M-20), p27 (F-8), mitogen-activated protein kinase kinase 7 (MKK7; MEK7), and IKK2 (H-470) were purchased from Santa Cruz Biotechnology (Santa Cruz, CA, USA). Antibodies against β-actin (AC-15) were purchased from Sigma Chemical (St Louis, MO, USA). DMEM and FBS were also purchased from Sigma Chemical. αMEM was purchased from Life Technologies (Rockville, MD, USA).

Cell culture and osteoclast differentiation assay

The RAW264.7 cell line was purchased from the Riken Cell Bank (Tsukuba, Japan). The cells were inoculated at 5×10^4 cells in a 6-well plate or 5×10^5 cells in a 10-cm plate and were cultured with DMEM containing 10% FBS at 37°C in 5% CO_2 in air. For osteoclast differentiation assay, RAW cells were grown in DMEM containing 10% FBS for 16–24 h. The culture medium was changed to DMEM containing 0.5% FBS, and the cells were cultured under serum starvation for 24–48 h. The growth-arrested RAW cells were stimulated with 10% FBS in the presence or absence of RANKL (100 ng/ml) for 1–7 days, fixed with 3.7% (vol/vol) formaldehyde in PBS), and stained at pH 5.0 in the presence of L(+)-tartaric acid using 3-hydroxy-2-naphthoic acid 2,4-dimethylanilide phosphate (Sigma) in *N,N*-dimethyl formamide (Sigma) as the substrate. $TRACP^+$ cells containing more than three nuclei were counted as osteoclasts.

For studies on primary osteoclast precursors, we used the M-CSF–dependent bone marrow macrophage (M-BMMϕ) culture system as described previously.[26] Briefly, bone marrow cells from 8-week-old male ddY mice (Sankyo Laboratories Animal Center, Tokyo, Japan) were seeded at 2×10^6 cells in a 6-multiwell plate and cultured in αMEM containing 10% FBS with M-CSF (10 ng/ml). After 2 days, adherent cells were used as M-BMMϕ after washing out the nonadherent cells including lymphocytes. The cells were then cultured in αMEM containing 0.5% FBS for 24 h and were further cultured in the presence of M-CSF (10 ng/ml) and RANKL (100 ng/ml) for 4 days. This experiment was performed according to the protocol approved by the Animal Care and Use Committee of the University of Tokyo.

Western blot analysis

Cells were rinsed with ice-cold PBS and lysed with RIPA buffer (100 μl for a well in 6-multiwell plate or 500 μl for a 10-cm plate) containing 10 mM Tris-HCl (pH 7.5), 150 mM NaCl, 1% Nonident-P40 (NP-40), 0.1% SDS, 10 μg/ml aprotinin, 0.1 M NaF, 2 mM Na_3VO_4, and 10 mM β-glycerophosphate. The cell lysates were sonicated briefly and clarified by centrifugation at 15,000*g* for 20 minutes at 4°C. The protein concentration in the cell lysate was measured using a Protein Assay Kit II (Bio-Rad). Equivalent amounts (10 μg) of cell lysate were electrophoresed by 7.5%, 10%, or 12.5% SDS-PAGE according to the molecular size of the proteins to be detected and were electrotransferred to polyvinylidene difluoride membranes (Immobilon-P; Millipore, Bedford, MA, USA). After blocking nonspecific binding with 5% skim milk, proteins were immunoblotted with respective antibodies and visualized using the ECL Plus Western Blotting Detection System (Amersham Pharmacia Biotech, Buckinghamshire, UK), following the manufacturer's instructions. Signals were quantified by densitometry (Bio-Rad). Experiments were performed at least three times, and a representative blotting was presented.

Transduction of $IKK2^{DN}$ and $MKK7^{DN}$ using adenovirus

The recombinant adenovirus vectors carrying the *$IKK2^{DN}$* (Ser177 and Ser181 to Ala; $AxIKK2^{DN}$) and the *β-galactosidase* gene (AxLacZ) were kindly provided by Inder Verma (Salk Institute, La Jolla, CA, USA) and Izumu Saito (Tokyo University), respectively. The recombinant

adenovirus vector carrying kinase negative MKK7 ($AxMKK7^{DN}$, replaced ATP-binding lysine with glutamate residue) was constructed as described.[21] Preparation and infection of $AxIKK2^{DN}$, $AxMKK7^{DN}$, and AxLacZ were performed as previously reported.[21] Titers of the viral stock were determined by modified endpoint cytopathic effect assay with the following modifications. Fifty microliters of DMEM containing 10% FBS was dispensed into each well of a 96-well tissue culture plate, and eight rows of 3-fold serial dilutions of the virus starting from 10^{-4} dilutions were prepared. HEK293 cells (3×10^5) in 50 μl of DMEM containing 10% FBS were added to each well. The plate was incubated at 37°C in 5% CO_2 in air, and 50 μl of DMEM containing 10% FBS was added to each well every 3 days. Twelve days later, the endpoint of the cytopathic effect was determined by microscopy, and the 50% tissue culture infectious dose ($TCID_{50}$) was calculated. One $TCID_{50}$ per milliliter approximately corresponds to one plaque-forming unit (PFU) per milliliter. The multiplicity of infection (MOI) is expressed as a measure of titer of how many PFUs are added to every cell. Infection of adenovirus vectors to RAW cells was carried out as follows. The cells were inoculated at the density of 5×10^4 cells per 6-well plate and incubated for 20 h with DMEM containing 10% FBS at 37°C. After further incubation with a small amount of DMEM containing the recombinant adenovirus for 2 h at 37°C at 100 MOI, the cells were washed twice with PBS and again incubated in DMEM containing 10% FBS. Experiments were performed 2 days after the infection.

Establishment of RAW cells stably transfected with Cdk6

RAW cells were inoculated at the density of 5×10^5 cells per 6-cm plate, incubated for 24 h, and transfected with pEF/neoI that carries human *Cdk6* cDNA[25] using LipofectAMINE reagent (Life Technologies) following the manufacturer's instructions. Twenty-four hours after transfection, the cells were passaged 1:10–1:100 into DMEM containing 10% FBS and 400 μg/ml G418 (Geneticin; Life Technologies) for stable expression. After colony formation, each colony was isolated and passaged. We picked up more than 100 drug-resistant colonies, each of which was derived from a single clone. The expression levels of Cdk6 were quantified by Western blotting, and 12 high-expressing clones and 10 low-expressing clones were established.

RT-PCR

Total RNA (1 μg) was extracted from RAW cells using ISOGEN (Wako Pure Chemicals, Osaka, Japan) following the manufacturer's instructions, reverse transcribed using SUPERSCRIPT First-Strand Synthesis System for RT-PCR (Life Technologies), and amplified within an exponential phase of the amplification with a Perkin Elmer PCR Thermal Cycler (PE-2400). Gene-specific primer pairs were as follows: 5′-GCAACCTCCAGTCAGCA-3′ and 5′-GAAGTCACAGCCCTCAGAATC-3′ for RANK and 5′-CATGTAGGCCATGAGGTCCACCAC-3′ and 5′-TGAAGGTCGGTGTGAACGGATTTGGC-3′ for GAPDH. The cycling parameters were 30 s at 94°C, 30 s at 49°C, and 90 s at 72°C for RANK and 30 s at 94°C, 30s at 55°C, and 90 s at 72°C for GAPDH. Each band intensity was quantified by densitometry (Bio-Rad).

Flow cytometric analysis

About 1×10^5 cells were suspended in 0.02 ml citrate buffer, to which was added 0.18 ml Soln. A (0.03 mg/ml trypsin, 3.4 mM trisodium citrate, 0.1% NP40, 1.5 mM Spermine 4 HCl, and 0.5 mM Tris-HCl [pH 7.6]) and incubated for 10 minutes, and then added with 0.15 ml Soln. B (3.4 mM trisodium citrate, 0.1% NP40, 1.5 mM Spermine 4 HCl, 0.5 mM Tris-HCl [pH 7.6], 0.5 mg/ml trypsin inhibitor, 0.1 mg/ml Ribonuclease A) and incubated for 10 minutes; 0.15 ml Soln. C (4.16 mg/ml propidium iodite, 3.4 mM trisodium citrate, 0.1% NP40, 4.8 mM Spermine 4 HCl, 0.5 mM Tris-HCl [pH 7.6]) was finally added, and the mixture was again incubated for 10 minutes. All procedures were performed at room temperature. The DNA content was analyzed by EPICS XL (Beckman), and the data were analyzed by XL EXPO32 (Beckman).

BrdU incorporation assay

RAW cells were inoculated at a density of 1×10^3 cells per well in a 96-well plate and cultured in DMEM containing 10% FBS with or without hRANKL (100 ng/ml). At 3 days of culture, cells were labeled with BrdU for 2 h, and cell proliferation was determined by BrdU incorporation using a kit (Cell Proliferation ELISA; Roche Molecular Biochemical, Mannheim, Germany) following the manufacturer's instructions.

Statistical analysis

Means of groups were compared by ANOVA, and significance of differences was determined by posthoc testing using the Bonferroni method.

RESULTS

Cdk6 is downregulated by RANKL in RAW cells

We initially confirmed that RAW cells differentiated into $TRACP^+$ multinucleated osteoclasts after 5 days of treatment with soluble RANKL (100 ng/ml; Fig. 1A). We analyzed the regulation by RANKL of cell cycle factors that critically regulate the onset of S phase: Cdk2, Cdk4, Cdk6, cyclins (D1, D2, D3, and E), and CKIs (p18, p21, and p27) in RAW cells (Figs. 1B and 1C). Western blot analysis revealed that the Cdk6 protein level was decreased by RANKL after 5 days of culture and thereafter, whereas those of cyclins were hardly affected throughout the culture period up to 7 days. Although Cdk4 and Cdk6 have about 70% homology of amino acid sequence[27] and share D cyclins as their catalytic partners, only Cdk6 was regulated by RANKL. Levels of Cdk2, p18, and p27 were somewhat decreased by RANKL treatment, and neither p21 nor p57 was detected throughout the experiments in this cell line (data not shown).

To investigate whether the Cdk6 downregulation is specific to this cell line or a more general phenomenon, we performed the same Western blot analysis with a culture of

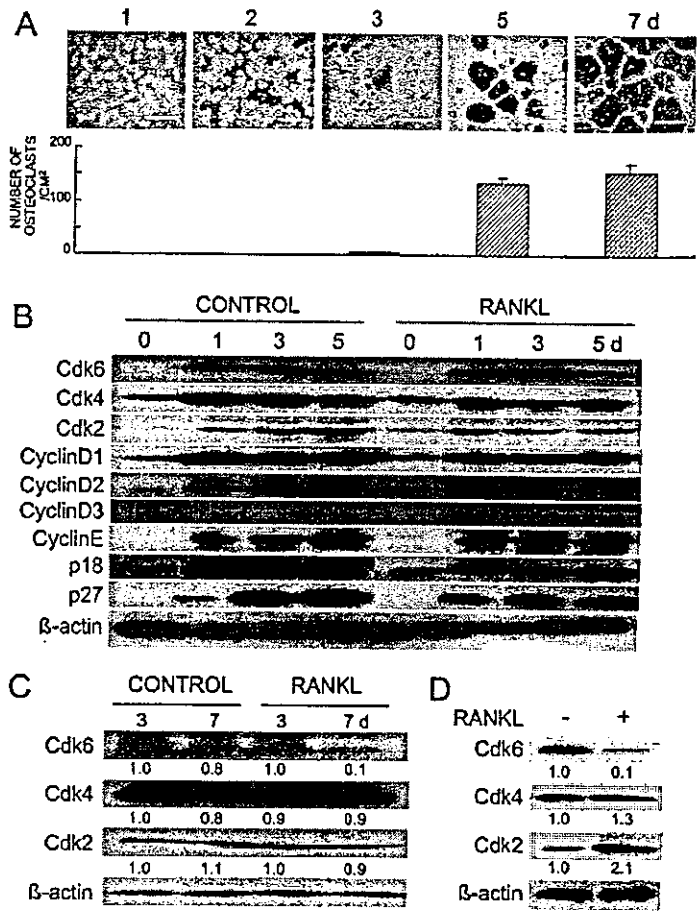

FIG. 1. (A) Time course of osteoclastogenesis from murine monocytic RAW264.7 cells, (B and C) expression of cell cycle factors by RANKL in the RAW264.7 cell culture, and (D) the murine primary osteoclast precursor M-BMMϕ culture. Cells were stimulated with serum in the presence or absence of RANKL (100 ng/ml) for the indicated days. (A) Osteoclastogenesis formed from cultured RAW cells was determined by TRACP staining, and the number of positively stained cells containing more than three nuclei was counted. Bar, 400 μm. The graph is expressed as means (bars) ± SE (error bars) for 8 wells/group. (B–D) The protein levels of cell cycle factors controlling the G1-S transition were determined at the indicated days of culture by Western blot analysis. β-actin was used as a loading control. B and C are from different cultures of RAW cells to confirm the regulation of Cdk's. D is from the M-BMMϕ culture for 4 days. The number under each band is the treated/control ratio of the intensity of each band normalized to that of β-actin measured by densitometry. In each figure a representative blotting was shown among at least three independent experiments that showed similar results.

primary osteoclast precursor M-BMMϕ. Treatment with RANKL inhibited induction of Cdk6 at 4 days, whereas Cdk4 was uninfluenced (Fig. 1D). Cdk2 was not decreased but was rather increased in this culture system. These results show that Cdk6 was specifically downregulated during the commitment to RANKL-induced osteoclast differentiation.

NF-κB mediates RANKL-induced downregulation of Cdk6

To examine the mediation of the NF-κB pathway, a major signaling pathway of RANKL, in the downregulation of Cdk6, we overexpressed $IKK2^{DN}$ in RAW cells using an adenovirus vector and examined its effect on RANKL-led Cdk6 downregulation. In our previous report, we confirmed that the adenovirus vector could efficiently transduce the $IKK2^{DN}$ gene into RAW cells and specifically suppressed the NF-κB activation in response to RANKL.[21] Both the inhibition of Cdk6 and the induction of osteoclastogenesis by RANKL were markedly reversed by the $IKK2^{DN}$ overexpression in RAW cells, whereas the control LacZ adenovirus infection did not affect the RANKL actions (Fig. 2A). These results indicate that the NF-κB signaling mediates not only osteoclast differentiation, but also the Cdk6 downregulation by RANKL.

We further investigated the possible involvement of the c-*jun* N-terminal kinase (JNK), another major signaling pathway of RANKL, in the downregulation of Cdk6 by RANKL. We previously reported that MKK7 is a vital function in JNK activation and osteoclast formation induced by RANKL, because $MKK7^{DN}$ overexpression using an adenovirus vector suppressed both of them.[21] Thus, we examined the effect of the adenovirus-mediated $MKK7^{DN}$ overexpression on RANKL-led Cdk6 downregulation in RAW cells. The $MKK7^{DN}$ overexpression suppressed the induction of osteoclastogenesis by RANKL as previously reported[21]; however, it did not restore the inhibition of Cdk6 in response to RANKL, unlike $IKK2^{DN}$ overexpression (Fig. 2B), indicating that the RANKL-led Cdk6 downregulation was not mediated by the JNK signaling.

RAW cells overexpressing Cdk6 resist RANKL-induced differentiation

As shown above, Cdk6 downregulation occurred during RANKL-induced osteoclast differentiation. Consequently, a critical question is whether or not this downregulation is essential for osteoclast differentiation. To address this, we generated RAW cell clones stably expressing various levels of Cdk6 by transfecting with an expressing vector harboring

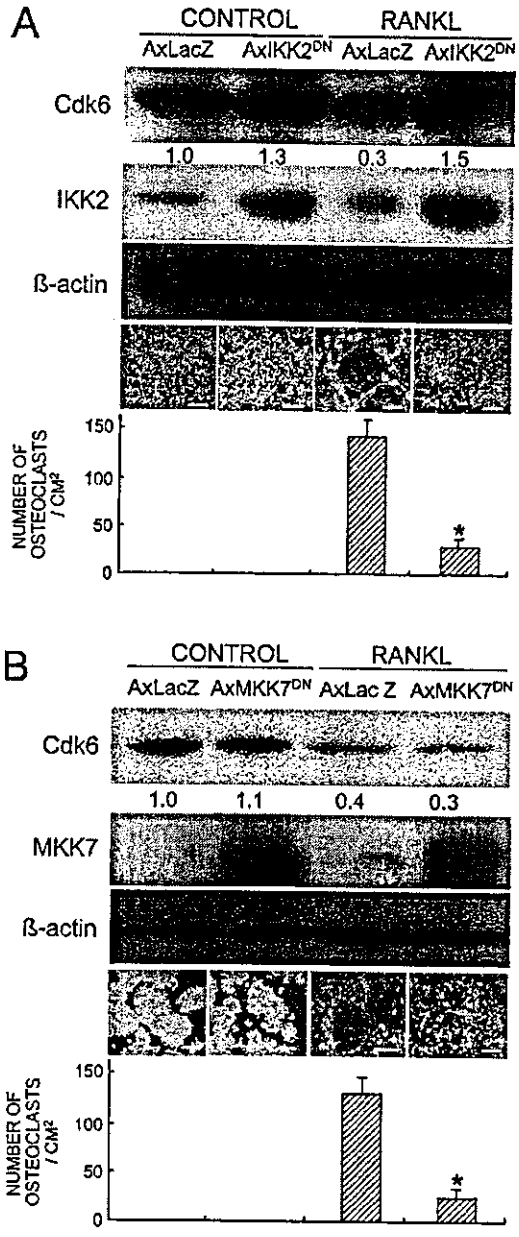

FIG. 2. Effects of overexpression of (A) IKK^{DN} and (B) $MKK7^{DN}$ using adenovirus vectors on the Cdk6 inhibition and osteoclastogenesis by RANKL in the RAW cell culture. RAW cells were infected with a recombinant adenovirus carrying the IKK^{DN}, $MKK7^{DN}$, or *LacZ* gene at 100 MOI, and subsequently, growth-arrested by incubation in a low serum medium for 2 days. The cells were stimulated with serum in the presence or absence of RANKL (100 ng/ml) for 5 days. Bar, 100 μm. Expressions of Cdk6, IKK2, and MKK7 were determined by Western blotting with β-actin as loading controls. The number under each band is the treated/control ratio of the intensity of the Cdk6 band normalized to that of β-actin measured by densitometry. Similar results were obtained in independent Western blottings of three separate experiments. The graph indicates means (bars) ± SE (error bars) for 8 wells/group. *Significant difference from the RANKL-treated and AxLacZ-infected culture; $p < 0.01$.

Cdk6 cDNA and tested their ability to respond to RANKL and differentiate to osteoclasts. The ability of RANKL to induce $TRACP^+$ multinucleated osteoclast formation was compared among the empty vector-transfected cells and low- (~1.5-fold) and high- (>5-fold) expressing cells. RANKL induced osteoclastogenesis in the empty vector-transfected cells and low-expressing clones; however, it was markedly decreased in high-expressing clones (Fig. 3A). Cdk6-led resistance to osteoclast differentiation is unlikely to be caused by an unexpected interference of the RANKL/NF-κB signaling by the overexpressed Cdk6, because RANK expression was not significantly affected by Cdk6 expression (Fig. 3B).

Overexpression of Cdk6 does not influence cell cycle regulation of osteoclasts

Because Cdk6 promotes the G1-S transition, suppression of osteoclast differentiation by overexpressed Cdk6 could be a mere consequence of its execution of this role. We therefore examined the effects of both RANKL and Cdk6 overexpression on G1-S transition and proliferation of RAW cells. The three kinds of transfected cells were similarly arrested in quiescence, stimulated with serum in the presence and absence of RANKL, and analyzed for cell proliferation and populations in G0/G1 and G2/M by BrdU incorporation and flow cytometric analysis (FACS; Table 1). At 3 days of culture, when osteoclastogenesis just started, RANKL slightly reduced cell proliferation and the G2/M population; however, Cdk6 overexpression caused no significant changes in either of them. These results indicate that the inhibitory effect of Cdk6 on osteoclast differentiation was not exerted through cell cycle regulation.

DISCUSSION

This study showed that Cdk6 is a key molecule in determining the differentiation rate of osteoclasts as a downstream effector of RANKL/NF-κB signaling. Figure 4 shows the mechanism of effect of RANKL on osteoclast differentiation based on present and previous studies. The RANK activation by binding of RANKL stimulates the NF-κB signaling, probably through association with TRAFs.[6,8–11] NF-κB moves from the cytoplasm into the nucleus, associates with various transcription factors in the nucleus, and downregulates Cdk6, which is a negative regulator of the transition from the G1 to the differentiation stage.

This study failed to show the contribution of JNK, another major pathway lying downstream of RANKL, to the RANKL-led Cdk6 downregulation. Our results, however, do not rule out the possibility that pathways other than NF-κB–mediated Cdk6 inhibition are required for osteoclast differentiation. JNK is known to activate activator protein 1 (AP-1), which is composed of various combinations of Fos and Jun family members. Mice deficient in c-*Fos* are reported to be osteopetrotic because of the failure in osteoclast differentiation, which can be rescued by Fra-1 as well as c-*Fos* overexpression,[28–31] indicating a crucial role of the JNK/AP-1 signaling in osteoclastogenesis.[12,13] JNK is activated by the phosphorylation of Thr and Tyr residues through MKK4 and/or MKK7. MKK7 seems to be

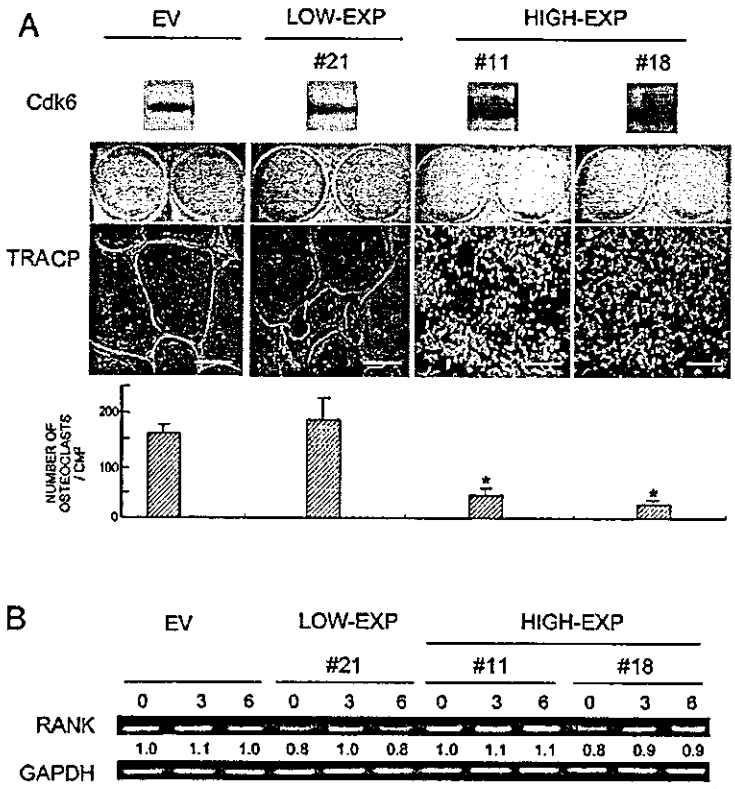

FIG. 3. (A) RANKL-induced osteoclastogenesis from RAW cells overexpressing Cdk6. Stable clones of RAW cells transfected with *Cdk6* cDNA were established as described in the Materials and Methods section, and clones with low expression (21) and high expression (11 and 18) were selected on Western blotting (top panel). These clones and empty vector-transfected RAW (EV) cells were induced for osteoclast differentiation by treating with RANKL (100 ng/ml) for 7 days, and osteoclast formation was determined by TRACP staining. The macroscopic images of culture wells and the microscopic images inside the wells are shown in the middle panels. Bar, 100 μm. The graph in the bottom panel is expressed as means (bars) $\pm$ SE (error bars) for 8 wells/group. *Significant difference from the EV cell culture; $p < 0.01$. (B) RANK mRNA levels by RT-PCR in each clone stimulated for 3 and 6 days with RANKL. The number under each band is the intensity of the RANK band normalized to that of GAPDH measured by densitometry. Other clones with low and high expressions showed similar results.

TABLE 1. CELL CYCLE REGULATION OF RAW CELLS OVEREXPRESSING Cdk6

	BrdU (OD)		*FACS*			
			G0/G1 (%)		*G2/M (%)*	
	RANKL⁻	*RANKL⁺*	*RANKL⁻*	*RANKL⁺*	*RANKL⁻*	*RANKL⁺*
EV	0.52 ± 0.03	0.39 ± 0.03*	75.2 ± 0.5	78.7 ± 0.7	15.9 ± 0.6	12.3 ± 0.6†
#21 (Low)	0.52 ± 0.05	0.34 ± 0.04*	75.5 ± 0.2	78.0 ± 0.4	16.1 ± 0.5	12.6 ± 0.5†
#11 (High)	0.56 ± 0.10	0.45 ± 0.03†	74.8 ± 0.9	78.9 ± 0.7	16.3 ± 0.9	12.2 ± 0.8†
#18 (High)	0.56 ± 0.08	0.39 ± 0.06†	75.7 ± 0.6	77.9 ± 0.9	16.7 ± 1.1	11.9 ± 0.6†

Cell proliferation was determined by BrdU incorporation into EV, low-expressing and high-expressing clones in the presence and absence of RANKL at 3 days of culture. Cell cycle distribution of mononuclear cells was determined by FACS, and percentages of cells in each cell cycle stage (G0/G1 and G2/M) are shown. Data are expressed as the mean ± SD for 6 wells/clone. Cdk6 overexpression did not significantly affect the cell proliferation and the cell cycle distribution. RANKL treatment reduced the cell proliferation and the cell population at G2/M.

*$p < 0.001$; †$p < 0.01$ significant inhibition by RANKL.

more specific in JNK activation than MKK4 because MKK4 is known to activate p38 MAPK as well. We previously reported that overexpression of $MKK7^{DN}$ in RAW cells by the adenovirus vector inhibited both RANKL-induced JNK activation and osteoclast formation.[21] JNK may possibly contribute to osteoclast differentiation through an independent pathway of Cdk6. Other possible pathways for osteoclast differentiation are the p38 MAPK and the Smad signaling. Recently, Matsumoto et al.[32] reported that RANKL activates p38 pathways in osteoclast precursors, which is essential for osteoclast differentiation, and Fuller et al.[33] and Kaneda et al.[34] showed the critical role of transforming growth factor (TGF)-β in osteoclast differentiation and survival. The involvement of cell cycle factors in osteoclast differentiation mediated by these pathways should be clarified in the future.

Cdk6 overexpression did not affect cell cycle regulation of RAW cells. D cyclins and partner kinases Cdk4 and Cdk6 are all known to be critical factors that control the cell growth potential,[35,36] but several specific roles have been reported for Cdk6. The Cdk6-cyclin D3 complex is unique among cyclin D and cognate kinase combinations and

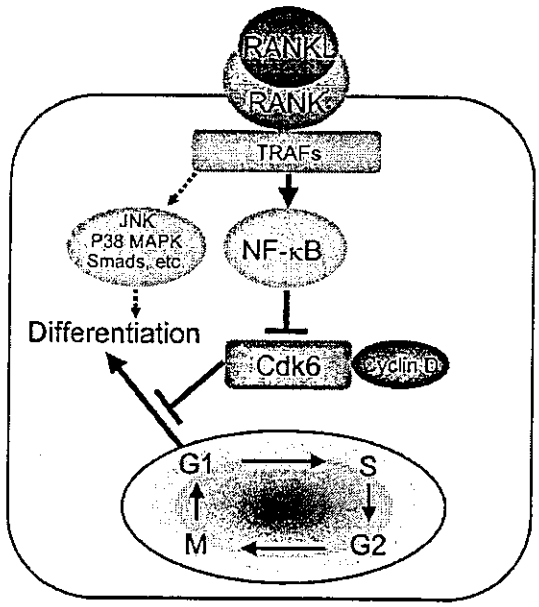

FIG. 4. Scheme of Cdk6-dependent RANKL effect on osteoclast differentiation obtained from this study. RANKL stimulates NF-κB signaling by binding to RANK through association with TRAFs. NF-κB downregulates Cdk6, which is a negative regulator of the transition from the G1 phase to the differentiation stage. Other signaling pathways such as JNK, p38 MAPK, and Smads might be involved in osteoclast differentiation through mechanisms independent of Cdk6.

evades inhibition by CKIs.[25] Therefore, it can greatly enhance the proliferative potential of fibroblasts under growth-suppressive conditions,[25] and consequently, sensitizes cells to physical and chemical transformation.[37] Cdk6 combined with cyclin K, encoded by human herpes virus 8, which is the causative agent of Kaposi sarcoma, is also reported to be immune to inhibition by CKIs.[38] These functions were not seen in Cdk4 complexes. This study discovered a novel function of Cdk6 as an inhibitor of the transition to the differentiation stage without affecting cell cycle regulation. Although Cdk4 has 70% homology of amino acid sequence with Cdk6,[27] the Cdk4 protein was not affected by RANKL in this study. We hereby propose that Cdk4 and Cdk6 play different roles and that Cdk4 cannot substitute for Cdk6 in osteoclastic cells.

How could Cdk6 control differentiation without influencing cell cycling? One possibility is that Cdk6 directly controls a factor critically involved in differentiation. This possibility may not be as remote as generally thought. In fission yeast, Pas1 cyclin and its partner kinase Pef1 activate a transcription factor complex functionally equivalent to E2F-DP of mammals, thereby promoting S phase entry, just like Cdk6, yet they independently inhibit the mating pheromone signaling whose activation is essential for differentiation of this yeast cell.[39] Thus, this might be a good model for the situation of Cdk6 in RANKL-induced osteoclast differentiation, highlighting a potential functional similarity between Cdk6 and Pef1.

Among cell cycle factors, Cdk's have vital roles in controlling cell cycle progression. Therefore, much attention has been devoted to the view that CKI-led inhibition of G1-specific Cdk's is critical for cell differentiation. Accordingly, potential roles for CKIs in differentiation have been studied extensively, but with mixed results.[40,41] Several studies revealed a certain correlation between induction of $p21^{CIP1}$ and differentiation in hematopoietic cells including monocytes/macrophages.[42–46] For osteoclast differentiation as well, upregulation of $p21^{CIP1}$ and $P27^{KIP1}$ is reported to be associated with osteoclast differentiation in the M-BMMϕ culture.[47] This was inconsistent with the present results in RAW cells that $P27^{KIP1}$ was not increased, but rather decreased, by RANKL and that $p21^{CIP1}$ could not be detected. Mice completely ablated for $p21^{CIP1}$ and/or $P27^{KIP1}$ or other major CKIs still develop and grow normally without significant bone abnormality such as osteopetrosis, strongly dismissing the current view.[41,48] Although there is evidence for $p57^{KIP2}$ being involved in differentiation of some cells,[49,50] no one has identified cell cycle factors that are controlled by differentiation signals and critically influence the differentiation commitment process. Because the Cdk6 downregulation was reproducible in RAW cell and M-BMMϕ cultures, we believe that Cdk6 generally plays a role in the RANKL-induced osteoclast differentiation. Although we tried to perform the signaling and overexpression experiments in M-BMMϕ, adenovirus infection and plasmid transfection were much less efficient in transducing these cells. Matsuo et al.[31] reported an efficient gene transfer into osteoclast precursors using a retrovirus vector system. However, the level of gene expression by retrovirus vectors is not enough for experiments using dominant negative molecules like this study. Developing more efficient gene transduction systems to primary osteoclast precursors will be helpful for further analysis of the signaling pathways of osteoclast differentiation.

This study for the first time showed that Cdk6, a G1 cell cycle factor, plays a critical role in controlling RANKL-induced osteoclast differentiation. Numerous signaling molecules, including transcription factors such as a nuclear factor of activated T-cells (NFATs),[51,52] have recently been reported to be involved in osteoclast differentiation. Consequently, one of these factors may be responsible for the RANKL-triggered repression of Cdk6 transcription. Identification of the transcriptional repressor as well as key targets for Cdk6 will definitely be required for deeper understanding of the molecular basis of bone resorption.

ACKNOWLEDGMENTS

We thank Reiko Yamaguchi for providing expert technical assistance and Drs Inder Verma and Izumu Saito for kindly providing adenovirus vectors carrying $IKK2^{DN}$ and LacZ, respectively. This study was funded by a Grant-in-Aid for Scientific Research from the Japanese Ministry of Education, Science, Sports, Culture and Technology (14657358).

REFERENCES

1. Suda T, Takahashi N, Udagawa N, Jimi E, Gillespie MT, Martin TJ 1999 Modulation of osteoclast differentiation and function by the new members of the tumor necrosis factor receptor and ligand families. Endocr Rev 20:345–357.
2. Lacey DL, Timms E, Tan HL, Kelley MJ, Dunstan CR, Burgess T, Elliott R, Colombero A, Elliott G, Scully S, Hsu H, Sullivan J, Hawkins N, Davy E, Capparelli C, Eli A, Qian YX, Kaufman S, Sarosi I, Shalhoub V, Senaldi G, Guo J, Delaney J, Boyle WJ 1998 Osteoprotegerin ligand is a cytokine that regulates osteoclast differentiation and activation. Cell 93:165–176.
3. Yasuda H, Shima N, Nakagawa N, Yamaguchi K, Kinosaki M, Mochizuki S, Tomoyasu A, Yano K, Goto M, Murakami A, Tsuda E, Morinaga T, Higashio K, Udagawa N, Takahashi N, Suda T 1998 Osteoclast differentiation factor is a ligand for osteoprotegerin/osteoclastogenesis-inhibitory factor and is identical to TRANCE/RANKL. Proc Natl Acad Sci USA 95:3597–3602.
4. Kong YY, Boyle WJ, Penninger JM 1999 Osteoprotegerin ligand: A common link between osteoclastogenesis, lymph node formation and lymphocyte development. Immunol Cell Biol 77:188–193.
5. Kong YY, Yoshida H, Sarosi I, Tan HL, Timms E, Capparelli C, Morony S, Oliveira-dos-Santos AJ, Van G, Itie A, Khoo W, Wakeham A, Dunstan CR, Lacey DL, Mak TW, Boyle WJ, Penninger JM 1999 OPGL is a key regulator of osteoclastogenesis, lymphocyte development and lymph-node organogenesis. Nature 397:315–323.
6. Li J, Sarosi I, Yan XQ, Morony S, Capparelli C, Tan HL, McCabe S, Elliott R, Scully S, Van G, Kaufman S, Juan SC, Sun Y, Tarpley J, Martin L, Christensen K, McCabe J, Kostenuik P, Hsu H, Fletcher F, Dunstan CR, Lacey DL, Boyle WJ 2000 RANK is the intrinsic hematopoietic cell surface receptor that controls osteoclastogenesis and regulation of bone mass and calcium metabolism. Proc Natl Acad Sci USA 97:1566–1571.
7. Nakagawa N, Kinosaki M, Yamaguchi K, Shima N, Yasuda H, Yano K, Morinaga T, Higashio K 1998 RANK is the essential signaling receptor for osteoclast differentiation factor in osteoclastogenesis. Biochem Biophys Res Commun 253:395–400.
8. Darnay BG, Haridas V, Ni J, Moore PA, Aggarwal BB 1998 Characterization of the intracellular domain of receptor activator of NF-κB (RANK). Interaction with tumor necrosis factor receptor-associated factors and activation of NF-κB and c-Jun N-terminal kinase. J Biol Chem 273:20551–20555.
9. Darnay BG, Ni J, Moore PA, Aggarwal BB 1999 Activation of NF-κB by RANK requires tumor necrosis factor receptor-associated factor (TRAF) 6 and NF-kappaB-inducing kinase. Identification of a novel TRAF6 interaction motif. J Biol Chem 274: 7724–7731.
10. Galibert L, Tometsko ME, Anderson DM, Cosman D, Dougall WC 1998 The involvement of multiple tumor necrosis factor receptor (TNFR)-associated factors in the signaling mechanisms of receptor activator of NF-kappaB, a member of the TNFR superfamily. J Biol Chem 273:34120–34127.
11. Lomaga MA, Yeh WC, Sarosi I, Duncan GS, Furlonger C, Ho A, Morony S, Capparelli C, Van G, Kaufman S, van der Heiden A, Itie A, Wakeham A, Khoo W, Sasaki T, Cao Z, Penninger JM, Paige CJ, Lacey DL, Dunstan CR, Boyle WJ, Goeddel DV, Mak TW 1999 TRAF6 deficiency results in osteopetrosis and defective interleukin-1, CD40, and LPS signaling. Genes Dev 13:1015–1024.
12. Iotsova V, Caamano J, Loy J, Yang Y, Lewin A, Bravo R 1997 Osteopetrosis in mice lacking NF-kappaB1 and NF-kappaB2. Nat Med 3:1285–1289.
13. Franzoso G, Carlson L, Xing L, Poljak L, Shores EW, Brown KD, Leonardi A, Tran T, Boyce BF, Siebenlist U 1997 Requirement for NF-kappaB in osteoclast and B-cell development. Genes Dev 11:3482–3496.
14. Verma IM, Stevenson J 1997 IkappaB kinase: Beginning, not the end. Proc Natl Acad Sci USA 94:11758–11760.
15. Karin M 1999 The beginning of the end: IkappaB kinase (IKK) and NF-kappaB activation. J Biol Chem 274:27339–27342.
16. Ghosh S 1999 Regulation of inducible gene expression by the transcription factor NF-kappaB. Immunol Res 19:183–189.
17. Li Q, Van Antwerp D, Mercurio F, Lee KF, Verma IM 1999 Severe liver degeneration in mice lacking the IkappaB kinase 2 gene. Science 284:321–325.
18. Li Q, Lu Q, Hwang JY, Buscher D, Lee KF, Izpisua-Belmonte JC, Verma IM 1999 IKK1-deficient mice exhibit abnormal development of skin and skeleton. Genes Dev 13:1322–1328.
19. Li ZW, Chu W, Hu Y, Delhase M, Deerinck T, Ellisman M, Johnson R, Karin M 1999 The IKKbeta subunit of IkappaB kinase (IKK) is essential for nuclear factor kappaB activation and prevention of apoptosis. J Exp Med 189:1839–1845.
20. Rudolph D, Yeh WC, Wakeham A, Rudolph B, Nallainathan D, Potter J, Elia AJ, Mak TW 2000 Severe liver degeneration and lack of NF-kappaB activation in NEMO/IKKgamma-deficient mice. Genes Dev 14:854–862.
21. Yamamoto A, Miyazaki T, Kadono Y, Takayanagi H, Miura T, Nishina H, Katada T, Wakabayashi K, Oda H, Nakamura K, Tanaka S 2002 Possible involvement of IkappaB kinase 2 and MKK7 in osteoclastogenesis induced by receptor activator of nuclear factor kappaB ligand. J Bone Miner Res 17:612–621.
22. Sherr CJ 1994 G1 phase progression: Cycling on cue. Cell 79: 551–555.
23. Sherr CJ, Roberts JM 1999 CDK inhibitors: Positive and negative regulators of G1-phase progression. Genes Dev 13:1501–1512.
24. Vidal A, Koff A 2000 Cell-cycle inhibitors: Three families united by a common cause. Gene 247:1–15.
25. Kobayashi K, Takahashi N, Jimi E, Udagawa N, Takami M, Kotake S, Nakagawa N, Kinosaki M, Yamaguchi K, Shima N, Yasuda H, Morinaga T, Higashio K, Martin TJ, Suda T 2000 Tumor necrosis factor alpha stimulates osteoclast differentiation by a mechanism independent of the ODF/RANKL-RANK interaction. J Exp Med 191:275–286.
26. Lin J, Jinno S, Okayama H 2001 Cdk6-cyclin D3 complex evades inhibition by inhibitor proteins and uniquely controls cell's proliferation competence. Oncogene 20:2000–2009.
27. Meyerson M, Enders GH, Wu CL, Su LK, Gorka C, Nelson C, Harlow E, Tsai LH 1992 A family of human cdc2-related protein kinases. EMBO J 11:2909–2917.
28. Wang ZQ, Ovitt C, Grigoriadis AE, Mohle-Steinlein U, Ruther U, Wagner EF 1992 Bone and haematopoietic defects in mice lacking c-*fos*. Nature 360:741–745.
29. Johnson RS, Spiegelman BM, Papaioannou V 1992 Pleiotropic effects of a null mutation in the c-fos proto-oncogene. Cell 71: 577–586.
30. Grigoriadis AE, Wang ZQ, Cecchini MG, Hofstetter W, Felix R, Fleisch HA, Wagner EF 1994 c-Fos: A key regulator of osteoclast-macrophage lineage determination and bone remodeling. Science 266:443–448.
31. Matsuo K, Owens JM, Tonko M, Elliott C, Chambers TJ, Wagner EF 2000 Fosl1 is a transcriptional target of c-Fos during osteoclast differentiation. Nat Genet 24:184–187.
32. Matsumoto M, Sudo T, Saito T, Osada H, Tsujimoto M 2000 Involvement of p38 mitogen-activated protein kinase signaling pathway in osteoclastogenesis mediated by receptor activator of NF-kappa B ligand (RANKL). J Biol Chem 275:31155–31161.
33. Fuller K, Lean JM, Bayley KE, Wani MR, Chambers TJ 2000 A role for TGFbeta(1) in osteoclast differentiation and survival. J Cell Sci 113:2445–2453.
34. Kaneda T, Nojima T, Nakagawa M, Ogasawara A, Kaneko H, Sato T, Mano H, Kumegawa M, Hakeda Y 2000 Endogenous production of TGF-beta is essential for osteoclastogenesis induced by a combination of receptor activator of NF-kappaB ligand and macrophage-colony-stimulating factor. J Immunol 165:4254–4263.
35. Baldin V, Lucus J, Marcote MJ, Pagano M, Draetta G 1993 Cyclin D1 is a nuclear protein required for cell cycle progression in G_1. Genes Dev 7:812–821.
36. Hengstchlager M, Braun K, Soucek A, Miloloza E, Hengstchlager O 1999 Cyclin-dependent kinases at the G_1-S transition of the mammalian cell cycle. Mutat Res 436:1–9.
37. Chen Q, Lin J, Jinno S, Okayama H 2003 Overexpression of Cdk6-cyclin D3 highly sensitizes cells to physical and chemical transformation. Oncogene 22:992–1001.
38. Swanton C, Mann DJ, Fleckenstein B, Neipel F, Peters G, Jones N 1997 Herpes viral cyclin/Cdk6 complexes evade inhibition by CDK inhibitor proteins. Nature 390:184–187.
39. Tanaka K, Okayama H 2000 A pcl-like cyclin activates the Res2p-Cdc10p cell cycle "start" transcriptional factor complex in fission yeast. Mol Biol Cell 11:2845–2862.
40. Missero C, Di Cunto F, Kiyokawa H, Koff A, Dotto GP 1996 The absence of p21Cip1/WAF1 alters keratinocyte growth and differ-

entiation and promotes ras-tumor progression. Genes Dev 10: 3065–3075.
41. Deng C, Zhang P, Harper JW, Elledge SJ, Leder P 1995 Mice lacking p21CIP1/WAF1 undergo normal development, but are defective in G1 checkpoint control. Cell 82:675–684.
42. Steinman RA, Hoffman B, Iro A, Guillouf C, Liebermann DA, el-Houseini ME 1994 Induction of p21 (WAF-1/CIP1) during differentiation. Oncogene 9:3389–3396.
43. Schwaller J, Koeffler HP, Niklaus G, Loetscher P, Nagel S, Fey MF, Tobler A 1995 Posttranscriptional stabilization underlies p53-independent induction of p21WAF1/CIP1/SDI1 in differentiating human leukemic cells. J Clin Invest 95:973–979.
44. Freemerman AJ, Vrana JA, Tombes RM, Jiang H, Chellappan SP, Fisher PB, Grant S 1997 Effects of antisense p21 (WAF1/CIP1/MDA6) expression on the induction of differentiation and drug-mediated apoptosis in human myeloid leukemia cells (HL-60). Leukemia 11:504–513.
45. Liu M, Lee MH, Cohen M, Bommakanti M, Freedman LP 1996 Transcriptional activation of the Cdk inhibitor p21 by vitamin D3 leads to the induced differentiation of the myelomonocytic cell line U937. Genes Dev 10:142–153.
46. Muto A, Kizaki M, Yamato K, Kawai Y, Kamata-Matsushita M, Ueno H, Ohguchi M, Nishihara T, Koeffler HP, Ikeda Y 1999 1,25-dihydroxyvitamin D3 induces differentiation of a retinoic acid-resistant acute promyelocytic leukemia cell line (UF-1) associated with expression of p21(WAF1/CIP1) and p27(KIP1). Blood 93:2225–2233.
47. Okahashi N, Murase Y, Koseki T, Sato T, Yamato K, Nishihara T 2001 Osteoclast differentiation is associated with transient upregulation of cyclin-dependent kinase inhibitors p21(WAF1/CIP1) and p27(KIP1). J Cell Biochem 80:339–345.
48. Nakayama K, Ishida N, Shirane M, Inomata A, Inoue T, Shishido N, Horii I, Loh DY 1996 Mice lacking p27(Kip1) display increased body size, multiple organ hyperplasia, retinal dysplasia, and pituitary tumors. Cell 85:707–720.
49. Yan Y, Frisen J, Lee MH, Massague J, Barbacid M 1997 Ablation of the CDK inhibitor p57Kip2 results in increased apoptosis and delayed differentiation during mouse development. Genes Dev 11:973–983.
50. Zhang P, Liegeois NJ, Wong C, Finegold M, Hou H, Thompson JC, Silverman A, Harper JW, DePinho RA, Elledge SJ 1997 Altered cell differentiation and proliferation in mice lacking p57KIP2 indicates a role in Beckwith-Wiedemann syndrome. Nature 387:151–158.
51. Takayanagi H, Kim S, Koga T, Nishina H, Isshiki M, Yoshida H, Saiura A, Isobe M, Yokochi T, Inoue J, Wagner EF, Mak TW, Kodama T, Taniguchi T 2002 Induction and activation of the transcription factor NFATc1 (NFAT2) integrate RANKL signaling in terminal differentiation of osteoclasts. Dev Cell 3:889–901.
52. Ishida N, Hayashi K, Hoshijima M, Ogawa T, Koga S, Miyatake Y, Kumegawa M, Kimura T, Takeya T 2002 Large scale gene expression analysis of osteoclastogenesis in vitro and elucidation of NFAT2 as a key regulator. J Biol Chem 277:41147–41156.

Address reprint requests to:
Hiroshi Kawaguchi, MD, PhD
Department of Orthopaedic Surgery
Faculty of Medicine
University of Tokyo
Hongo 7-3-1, Bunkyo
Tokyo 113-8655, Japan
E-mail: kawaguchi-ort@h.u-tokyo.ac.jp

Received in original form August 10, 2003; in revised form February 5, 2004; accepted March 11, 2004.

MOLECULAR AND CELLULAR BIOLOGY, Aug. 2004, p. 6560–6568
0270-7306/04/$08.00+0 DOI: 10.1128/MCB.24.15.6560–6568.2004

Vol. 24, No. 15

Bone Morphogenetic Protein 2-Induced Osteoblast Differentiation Requires Smad-Mediated Down-Regulation of Cdk6

Toru Ogasawara,[1,2] Hiroshi Kawaguchi,[2] Shigeki Jinno,[1] Kazuto Hoshi,[2] Keiji Itaka,[2] Tsuyoshi Takato,[2] Kozo Nakamura,[2] and Hiroto Okayama[1]*

Departments of Biochemistry and Molecular Biology[1] and Sensory and Motor System Medicine,[2] The University of Tokyo Graduate School of Medicine, Tokyo 113-0033, Japan

Received 31 March 2004/Accepted 8 May 2004

Because a temporal arrest in the G_1 phase of the cell cycle is thought to be a prerequisite for cell differentiation, we investigated cell cycle factors that critically influence the differentiation of mouse osteoblastic MC3T3-E1 cells induced by bone morphogenetic protein 2 (BMP-2), a potent inducer of osteoblast differentiation. Of the G_1 cell cycle factors examined, the expression of cyclin-dependent kinase 6 (Cdk6) was found to be strongly down-regulated by BMP-2/Smads signaling, mainly via transcriptional repression. The enforced expression of Cdk6 blocked BMP-2-induced osteoblast differentiation to various degrees, depending on the level of its overexpression. However, neither BMP-2 treatment nor Cdk6 overexpression significantly affected cell proliferation, suggesting that the inhibitory effect of Cdk6 on cell differentiation was exerted by a mechanism that is largely independent of its cell cycle regulation. These results indicate that Cdk6 is a critical regulator of BMP-2-induced osteoblast differentiation and that its Smads-mediated down-regulation is essential for efficient osteoblast differentiation.

Bone morphogenetic protein 2 (BMP-2) is a potent inducer of bone formation through its stimulation of osteoblast differentiation (17). It exerts this effect via two types of serine/threonine kinase receptors: BMP-2 binds the type II receptor, which subsequently activates the type I receptor by a direct association. Signals from the activated type I receptor are transmitted to the nucleus through various mediator molecules, the most important among them being a family of proteins termed Smads. Smads are classified into three subgroups, i.e., Smad1, Smad5, and Smad8 are classified as receptor-regulated Smads (R-Smads), Smad4 is classified as a common-partner Smad (Co-Smad), and Smad6 and Smad7 are classified as inhibitory Smads (I-Smads) (6). R-Smads are directly activated by the type I receptor, form complexes with Co-Smad, and are translocated into the nucleus, where they regulate the transcription of target genes. I-Smads inhibit the activation of R-Smads by interfering with their association with the type I receptor, which results in the hindrance of the assembly of R-Smads with Co-Smad. Although the downstream signaling of the BMP-2/Smad pathway leading to osteoblast differentiation has been extensively investigated, most of the studies have focused on the bone-related transcriptional regulators Runx2/Cbfa1 (7, 31), osterix (12), SIP1 (25), Smurf1 (32), NF-κB (4, 9), Hoxc-8 (1, 20), and Tob (29).

The proliferation of eukaryotic cells depends on their progression through the cell cycle, and an at least temporal cell cycle arrest in the G_1 phase is thought to be a prerequisite for cell differentiation (18). Cell cycle progression is controlled by the action of cyclins and cyclin-dependent protein kinases (Cdks), which phosphorylate and thereby activate cell cycle factors that are essential for the onset of the next cell cycle phase. In mammalian cells, traverse through G_1 and subsequent S-phase entry require the activities of the cyclin D-dependent kinase Cdk4 and/or Cdk6 (11) and the cyclin E-dependent kinase Cdk2. A key physiological substrate for Cdk4 and Cdk6 is the retinoblastoma (Rb) protein, which binds and inactivates the E2F-DP transcription complexes that are essential for S-phase entry. Phosphorylation by Cdk4/6 and additionally by Cdk2 inactivates Rb, thereby releasing E2F-DP from inactivation and consequently promoting S-phase entry and progression (5, 14). These Cdks are negatively regulated by cyclin-dependent kinase inhibitors (CKIs) via direct binding to themselves (19, 26). CKIs have been classified into two families, the INK4 family and the Cip/Kip family. INK4 family members (p16, p15, p18, and p19) inhibit only Cdk4 and Cdk6, whereas Cip/Kip family members (p21, p27, and p57) inhibit all of the Cdks except for the Cdk6-cyclin D3 complex. Because of its unique ability to evade inhibition by Cip/Kip proteins, Cdk6-D3 can control the cell's proliferative potential under growth-suppressive conditions despite its relative minority in level of expression in mesenchymal cells (8).

Cdks play crucial roles in controlling cell cycle progression. Therefore, much attention has been attracted by the view that the CKI-led inhibition of G_1-specific Cdks is critical for cell differentiation. Accordingly, potential roles for CKIs in differentiation have been extensively studied, but with mixed results. Many studies revealed a certain correlation between the induction of $p21^{CIP1}$ and differentiation, yet many did not. Mice with a complete deletion of $p21^{CIP1}$ and/or $p27^{KIP1}$ or other major CKIs still develop normally, with proper differentiation, which calls the current view into question (3, 13). Although there is evidence for $p57^{KIP2}$ being involved in the differentiation of some cells (28, 30), no one has identified cell cycle factors that are controlled by differentiation signals and that critically influence the differentiation commitment process.

* Corresponding author. Mailing address: Department of Biochemistry and Molecular Biology, Graduate School and Faculty of Medicine, University of Tokyo, 7-3-1 Hongo, Bunkyo, Tokyo 113-0033, Japan. Phone: 81-3-5841-3440. Fax: 81-3-3815-1490. E-mail: okayama-tky@umin.ac.jp.

Since in lower eukaryotes the control of the cell cycle factors driving the onset of S phase greatly influences the commitment to cell differentiation, we reinvestigated the possibility of the crucial participation of some cell cycle start factors in mammalian cell differentiation control as well, using BMP-2-induced osteoblast differentiation as a model system, and we found that upon BMP-2 treatment, Cdk6 expression was down-regulated primarily by BMP-2/Smad signal-invoked transcriptional repression and that its down-regulation was essential for efficient osteoblast differentiation.

MATERIALS AND METHODS

Reagents and antibodies. Recombinant human BMP-2 was generously provided by Yamanouchi Pharmaceutical Co., Ltd. (Tokyo, Japan), and recombinant human fibroblast growth factor 2 (FGF-2) was provided by Kaken Pharmaceutical Co., Ltd. (Chiba, Japan). Antibodies against Cdk2 (H-298), Cdk4 (C-22), Cdk6 (C-21), Rb (C-15), cyclin D1 (C-20), cyclin D2 (M-20), cyclin D3 (C-16), cyclin E (M-20), p18 (M-20), p21 (H164), p27 (F-8), BMPRIA (E-16), BMPRII (T-18), and Smad6 (S-20) were obtained from Santa Cruz Biotechnology. Anti-phosphorylated Rb (G3-245) and anti-β-actin (AC-15) antibodies were purchased from Pharmingen and Sigma, respectively.

Osteoblast culture. The mouse osteoblast cell line MC3T3-E1 was purchased from the Riken Cell Bank (Tsukuba, Japan). Primary osteoblasts were isolated from neonatal mouse calvariae according to international and university guidelines (33). Calvariae dissected from 1- to 4-day-old mice were digested for 10 min with 1 ml of trypsin-EDTA (Sigma) containing 10 mg of collagenase (type 7; Sigma), and the released cells were collected. This step was repeated five times, and the cells obtained by the second through fifth digestion steps were pooled as primary osteoblasts. MC3T3-E1 cells and primary osteoblasts were maintained in α-modified minimum essential medium (α-MEM) (Life Technologies Inc.) containing 10% fetal bovine serum (FBS) (Sigma). The cells were inoculated at 5×10^4 cells in a six-well plate or 5×10^5 cells in a 10-cm-diameter plate and allowed to proliferate for 20 to 24 h, and then their growth was arrested by incubation for 24 to 48 h in α-MEM containing 0.5% FBS. Growth-arrested cells were then induced for differentiation or proliferation by stimulation with α-MEM containing 10% FBS and BMP-2 (300 ng/ml) or FGF-2 (10 nM). To block protein degradation, we added the proteasome inhibitor MG132 (*Z*-Leu-Leu-Leu-aldehyde; Peptide Institute, Osaka, Japan) to the culture medium to a final concentration of 2 μM, as described previously (15, 24).

Construction of cell clones constitutively expressing Cdk6. MC3T3-E1 cells were inoculated at 5×10^5 cells per 6-cm-diameter plate, incubated for 24 h, and then transfected with the pEF/neo I vector carrying a human *Cdk6* cDNA or no insert by use of the Lipofectamine reagent (Life Technologies, Inc.) according to the manufacturer's instructions. Twenty-four hours later, the cells were split 1:10 to 1:100 and selected in α-MEM containing 10% FBS and 200 μg of G418 (Geneticin; Life Technologies, Inc.)/ml. Stable G418-resistant colonies were then isolated and expanded for analysis. The levels of Cdk6 were then quantified by Western blotting to identify several high- and low-expression-level clones for in-depth analysis.

Smad6 expression and differentiation induction. MC3T3-E1 cells were inoculated at 5×10^4 cells per well in a six-well plate and incubated at 37°C for 20 h in α-MEM containing 10% FBS. The cells were then infected for 2 h with a recombinant adenovirus carrying *smad6* or *lacZ* at a multiplicity of infection of 100 PFU/cell, for which >80% of the cells were infected, as determined by staining for β-galactosidase. The cells were washed twice with phosphate-buffered saline (PBS), their growth was arrested by incubation in α-MEM containing 0.5% FBS for 48 h, and they were stimulated with α-MEM containing 10% FBS with or without BMP-2 (300 ng/ml).

Western blot analysis. The cells were rinsed with ice-cold PBS and lysed with RIPA buffer (10 mM Tris-HCl [pH 7.5], 150 mM NaCl, 1% Nonidet P-40 [NP-40], 0.1% sodium dodecyl sulfate [SDS], 10 μg of aprotinin/ml, 0.1 M NaF, 2 mM Na_3VO_4, and 10 mM β-glycerophosphate). After a brief sonication, the lysed cells were centrifuged at 15,000 × *g* for 20 min at 4°C to obtain soluble cell extracts. The cell extracts (10 μg of protein each) were separated by SDS–7.5, 10, or 12.5% polyacrylamide gel electrophoresis and electrotransferred to polyvinylidene difluoride membranes (Immobilon-P; Millipore Corp., Bedford, Mass.). After the blocking of nonspecific binding by soaking of the filters in 5% skim milk, the desired proteins were immunodetected with their respective antibodies, followed by visualization by use of the ECL Plus Western blotting detection system (Amersham Pharmacia Biotech, Buckinghamshire, United Kingdom) according to the manufacturer's instructions.

In vitro kinase assay. Cells were lysed with ice-cold IP buffer containing 50 mM HEPES (pH 7.5), 150 mM NaCl, 1 mM EDTA, 2.5 mM EGTA, 1 mM dithiothreitol, 0.1% Tween 20, 10% glycerol, 1 mM phenylmethylsulfonyl fluoride (PMSF), 10 μg of aprotinin/ml, 1 mM NaF, and 0.1 mM sodium orthovanadate. The lysates were incubated at 4°C for 2 h with 0.5 μg of the anti-Cdk4 or -Cdk6 antibody. Protein G-Sepharose (15 μl) (Amersham-Pharmacia) was then added and incubated for an additional 1 h. Immune complexes bound to protein G-Sepharose were precipitated by centrifugation and washed with glycerol-free IP buffer. The immunopurified Cdk4 or Cdk6 protein was incubated at 30°C for 30 min in R buffer (50 mM HEPES [pH 7.5], 2.5 mM EGTA, 10 mM KCl, 10 mM $MgCl_2$, 1 mM dithiothreitol) containing 0.5 μg of truncated Rb (Santa Cruz) and 10 mM ATP. The reaction products were electrophoresed in SDS–10% polyacrylamide gels and transferred to polyvinylidene difluoride membrane filters. Phosphorylated truncated Rb was detected with an anti-Ser780-phosphorylated Rb antibody (MBL).

Reverse transcription-PCR (RT-PCR). Total RNAs (1 μg) extracted from cells were reverse transcribed and amplified by PCR. The gene-specific primer pairs used were as follows: 5′-CGTGGTCAGGTTGTTTGATG-3′ and 5′-TGCGAAACATTTCTGCAAAG-3′ for Cdk6, 5′-ATGAGGACCCTCTCTCTGC T-3′ and 5′-CCGTAGATGCGTTTGTAGGC-3′ for osteocalcin, 5′-TAGCAC CAGAGGATACCTTGC-3′ and 5′-AATGCTTCATCCTGTTCCAAA-3′ for BMPRIA, 5′-CAGAATCAAGAACGGCTATG-3′ and 5′-TTGTTTACGGTC TCCTGTCA-3′ for BMPRII, and 5′-CATGTAGGCCATGAGGTCCACCA C-3′ and 5′-TGAAGGTCGGTGTGAACGGATTTGGC-3′ for glyceraldehyde-3-phosphate dehydrogenase. The cycling parameters were 30 s at 94°C, 30 s at 55°C, and 1 min 30 s at 72°C for Cdk6, osteocalcin, and glyceraldehyde-3-phosphate dehydrogenase; and 30 s at 94°C, 30 s at 53°C, and 1 min 30 s at 72°C for BMPRIA and BMPRII.

ALP activity measurement and in situ staining. MC3T3-E1 cells were inoculated at 5×10^4 cells per well in a six-well plate and cultured in α-MEM containing 10% FBS with or without BMP-2 (300 ng/ml). After being cultured for 3 days, the cells were rinsed with PBS and lysed by sonication in 10 mM Tris-HCl buffer (pH 8.0) containing 1 mM $MgCl_2$ and 0.5% Triton X-100. The alkaline phosphatase (ALP) activity in the lysates was measured by the hydrolysis of *p*-nitrophenyl phosphate to *p*-nitrophenol. The protein content was determined by using a protein assay kit (Bio-Rad). For in situ ALP staining, the cells were fixed with 3.7% (vol/vol) formaldehyde in PBS and were stained with naphthol AS-MX phosphate (Sigma), with *N,N*-dimethyl formamide as a substrate and Fast BB salt (Sigma) as a coupler.

BrdU incorporation assay. MC3T3-E1 cells were inoculated at 10^3 cells per well in a 96-well plate and cultured in α-MEM containing 10% FBS with or without BMP-2 (300 ng/ml). After being cultured for 1 or 3 days, the cells were labeled with bromodeoxyuridine (BrdU) for 2 h, and the cell population entering S phase was determined by quantifying the incorporated BrdU (Cell Proliferation ELISA; Roche Molecular Biochemical, Mannheim, Germany).

XTT assay. Cells were inoculated at 10^3 cells per well in a 96-well plate and cultured for 5 days in α-MEM containing 10% FBS with or without BMP-2 (300 ng/ml), with cell sampling every day. The sampled cells were quantified by use of an XTT {sodium 3,3-[(phenylamino)carbonyl]-3,4-tetrazolium-bis(4-methoxy-6-nitro) benzenesulfonic acid hydrate} assay kit (Roche).

Flow cytometric analysis. Approximately 10^5 cells were suspended in 0.02 ml of citrate buffer and subjected to the following serial treatments at room temperature: (i) the addition of 0.18 ml of solution A (0.03 mg of trypsin/ml, 3.4 mM trisodium citrate, 0.1% NP-40, 1.5 mM spermine 4HCl, and 0.5 mM Tris-HCl [pH 7.6]) and incubation for 10 min; (ii) the addition of 0.15 ml of solution B (3.4 mM trisodium citrate, 0.1% NP-40, 1.5 mM spermine-4HCl, 0.5 mM Tris-HCl [pH 7.6], 0.5 mg of trypsin inhibitor/ml, 0.1 mg of RNase A/ml) and incubation for 10 min; and (iii) the addition of 0.15 ml of solution C (4.16 mg of propidium iodide/ml, 3.4 mM trisodium citrate, 0.1% NP-40, 4.8 mM spermine 4HCl, 0.5 mM Tris-HCl [pH 7.6]) and incubation for 10 min. The DNA content was determined and analyzed with EPICS XL and XL EXPO32 instruments (Beckman).

ChIP. Chromatin immunoprecipitation (ChIP) was performed by use of a commercial kit (Upstate Cell Signaling Solutions, Lake Placid, N.Y.). Cells were inoculated at a density of 5×10^5 cells per 10-cm-diameter dish and cultured in α-MEM containing 10% FBS and BMP-2 (300 ng/ml). At days 1 and 4 of culture, the protein and DNA were cross-linked by the direct addition of formaldehyde to the culture medium to a final concentration of 1% and incubation at 37°C for 10 min. The cells were then washed twice with ice-cold PBS containing 1 mM PMSF and 1 μg of aprotinin/ml, collected with cell scrapers, sedimented by low-speed centrifugation, resuspended, and incubated at 4°C for 10 min in 200 μl

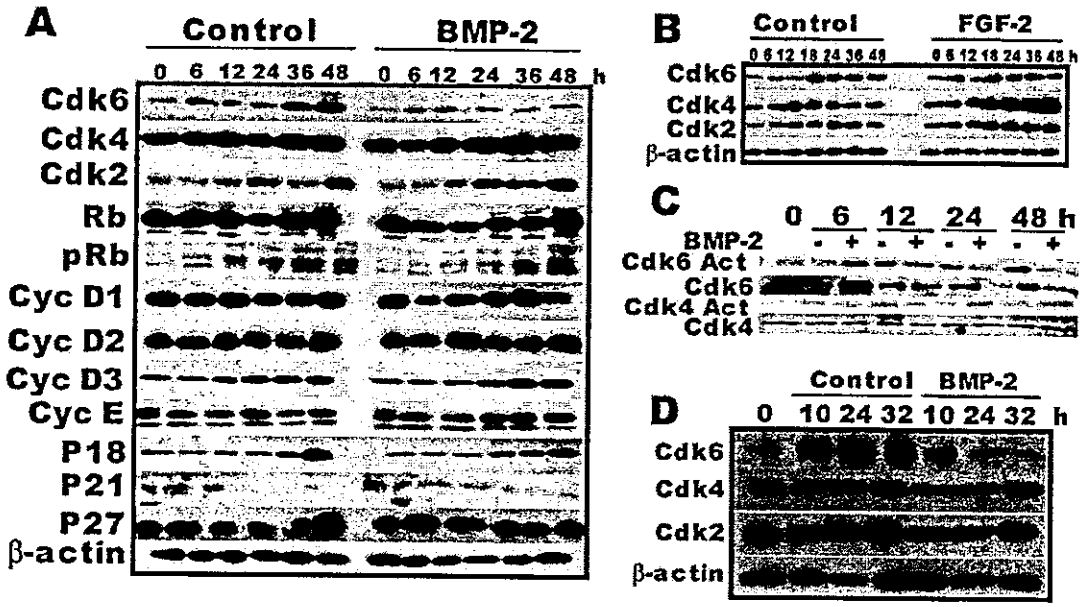

FIG. 1. BMP-2 treatment inhibits expression of Cdk6. (A) Time-dependent expression of cell cycle factors controlling the G_1-S transition in mouse osteoblastic MC3T3-E1 cells during differentiation induction. Growth-arrested MC3T3-E1 cells were stimulated with FBS in the presence or absence of BMP-2, with cell sampling done at the indicated times. The amounts of cell cycle factors expressed during stimulation were semiquantified by Western blotting. β-Actin was used as a loading control. Cyc, cyclin. (B) Time-dependent expression of Cdks 2, 4, and 6 in MC3T3-E1 cells during FGF-2 stimulation. Growth-arrested MC3T3-E1 cells were stimulated with FBS in the presence or absence of FGF-2, with cell sampling performed at the indicated times, followed by Western blotting of Cdks 2, 4, and 6. (C) Cdk6 and Cdk4 activities in MC3T3-E1 cells during stimulation with or without BMP-2. Cdk6 and Cdk4 were immunoprecipitated and assayed for kinase activity, and their amounts were determined in parallel. (D) Time-dependent expression of Cdk2, Cdk4, and Cdk6 proteins in primary neonatal mouse calvarial osteoblasts stimulated with or without BMP-2.

of lysis buffer (1% SDS, 10 mM EDTA, 50 mM Tris [pH 8.1]) containing 1 mM PMSF and 1 μg of aprotinin/ml. The cell lysates were then sonicated at 4°C with a Branson 450 sonifier at an output control of 2 and a duty cycle of 10 for 10 s to fragment the chromosomal DNA into 0.2- to 1-kb pieces. After the insoluble material was removed by centrifugation at 15,000 × *g* for 10 min, 1/10 aliquots of the supernatants were taken and saved as input. The rest of the supernatants were diluted appropriately with ChIP dilution buffer (0.01% SDS, 1.1% Triton X-100, 1.2 mM EDTA, 16.7 mM Tris-HCl [pH 8.1], 167 mM NaCl) containing 1 mM PMSF and 1 μg of aprotinin/ml and were pretreated with a salmon sperm DNA–protein A–50% agarose slurry at 4°C for 30 min with gentle agitation. After a brief centrifugation to remove the slurry, the supernatants were collected and incubated at 4°C overnight with antibodies (anti-mouse pRb [1 μg each of Ab-4 and Ab-5; Neomarkers] or anti-CBFA1 [2 μg of sc-8566; Santa Cruz]). Immunocomplexes were allowed to bind to protein A-agarose by incubation with a salmon sperm DNA-protein A–50% agarose slurry at 4°C for 1 h with gentle agitation. After a brief centrifugation, the supernatants were saved as the unbound fraction. The protein A-bound immunocomplexes were washed once with 1 ml each of the buffers shown below in sequential order: (i) low-salt immune complex wash buffer (0.1% SDS, 1% Triton X-100, 2 mM EDTA, 20 mM Tris-HCl [pH 8.1], 150 mM NaCl), (ii) high-salt immune complex wash buffer (0.1% SDS, 1% Triton X-100, 2 mM EDTA, 20 mM Tris-HCl [pH 8.1], 500 mM NaCl), (iii) LiCl immune complex wash buffer (0.25 M LiCl, 1% IGEPAL-CA630, 1% sodium deoxycholate, 1 mM EDTA, 10 mM Tris, pH 8.1), and (iv) TE buffer (10 mM Tris-HCl, 1 mM EDTA, pH 8.0). The protein A-bound immunocomplexes were resuspended in 250 μl of elution buffer (1% SDS, 0.1 M $NaHCO_3$), mixed by vortexing, and incubated at room temperature for 15 min, with gentle agitation. After a brief centrifugation, the supernatants were saved, and elution was repeated one more time. Both eluates were combined, and after the addition of 20 μl of 5 M NaCl, were heated at 65°C for 4 h to reverse cross-linking. Ten microliters of 0.5 M EDTA, 20 μl of 1 M Tris-HCl (pH 6.5), and 2 μl of proteinase K (20 mg/ml) were added to the eluates, and the mixtures were incubated for 1 h at 45°C to remove proteins bound to DNA, followed by sequential extraction steps with phenol-chloroform and chloroform and by DNA precipitation with ethanol after the addition of 10 μg of glycogen as a carrier. The precipitated DNA was recovered by centrifugation and resuspended in 100 μl of TE buffer. The input fractions of the supernatants and the unbound fractions were similarly treated to remove cross-links and proteins, and the DNAs were ethanol precipitated similarly and dissolved in 10 and 100 μl of TE buffer, respectively. The osteocalcin and myogenin promoter sequences were amplified by 40 cycles of PCR from 1 μl each of the DNA solutions, with parameters of 30 s at 95°C, 30 s at 60°C, and 30 s at 72°C and with the following primers: 5′-CTGAACTGGGCAAATGAGGACA-3′ and 5′-AGGGGATGCT GCCAGGACTAAT for the mouse osteocalcin promoter (positions −67 to −471) and 5′-ACCCCTTTCTTGTTCCCTTCCT-3′ and 5′-CTCCCGCAGCC CCTCAC-3′ for the mouse myogenin promoter (positions −9 to −431).

Statistical analysis. The means of groups were compared by analysis of variance, and the significance of differences was determined by post hoc testing using the Bonferroni method.

RESULTS

Cdk6 is down-regulated in osteoblasts upon BMP-2 treatment. Within 24 h after treatment with BMP-2, C2C12 cells begin to express osteocalcin mRNA and ALP, two representative markers of mature osteoblasts (21). Accordingly, the commitment to BMP-2-induced osteoblast differentiation occurs within 24 h. Since the MC3T3-E1 cells used in the present study are known to be in a stage that is one step more differentiated toward mature osteoblasts than C2C12 cells, we assumed that the commitment of this cell line to BMP-2-induced osteoblast differentiation occurred well within 24 h, and therefore we analyzed the effect of BMP-2 on the initial 48-h expression levels of cell cycle factors that critically regulate the onset of S phase in this cell line. The cells were arrested in quiescence by serum starvation, stimulated with serum in the presence or absence of BMP-2, and harvested every 6 or 12 h. The amounts of cyclins (D1, D2, D3, and E), Cdk2, Cdk4,

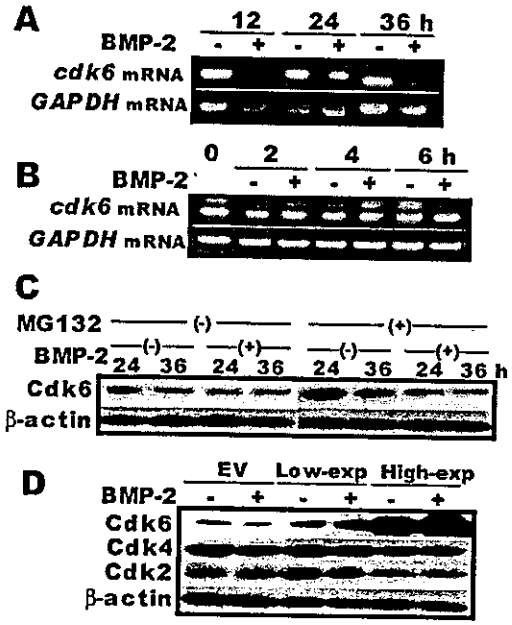

FIG. 2. BMP-2 down-regulates Cdk6 expression mainly via preventing transcription. (A) BMP-2 treatment markedly reduces *cdk6* mRNA level. Growth-arrested MC3T3-E1 cells were stimulated with or without BMP-2 for the indicated times, and RNAs were prepared. *cdk6* mRNA was semiquantified by RT-PCR. (B) BMP-2 treatment does not affect the stability of *cdk6* mRNA. Growth-arrested MC3T3-E1 cells were stimulated with serum for 6 h and then incubated with actinomycin D (Sigma) (0.1 μg/ml) with or without the addition of BMP-2. RNAs were prepared and the Cdk6 transcript was semiquantified by RT-PCR. Glyceraldehyde-3-phosphate dehydrogenase (GAPDH) mRNA was used as a control for the RNA preparations. (C) The proteasome inhibitor MG132 does not influence the action of BMP-2 on the Cdk6 protein level. Growth-arrested MC3T3-E1 cells were stimulated for 24 and 36 h with or without BMP-2 and/or MG132 (2 μM), and the Cdk6 protein levels were determined by Western blotting. (D) BMP-2 treatment does not affect the level of forcefully expressed Cdk6 protein. Clones constitutively expressing Cdk6 from an EF1α-promoter as well as empty vector-transfected MC3T3-E1 (EV) cells were growth arrested as described in the text and stimulated for 48 h with or without BMP-2. The amounts of Cdk6, Cdk4, and Cdk2 were then semiquantified by Western blotting.

Cdk6, CKIs (p18, p21, p27, and p57), and Rb and phosphorylated Rb proteins in the whole-cell lysate at each time point were analyzed by Western blotting (Fig. 1). In this cell line, the amounts of Cdk6, Cdk2, and p18 increased during serum stimulation, as early as 6 h after stimulation, and the amount of p21 decreased, whereas the amounts of the remaining factors were unchanged. This cell line did not express detectable amounts of p57 throughout the experiment (data not shown). Coinciding with the elevation of Cdk2, phosphorylated forms of the Rb protein appeared. Under these conditions, the cells grew to confluence but did not commit to differentiation into osteoblasts.

In contrast, when MC3T3-E1 cells were stimulated with BMP-2 to stimulate osteoblast differentiation, the induction of Cdk6 completely disappeared (Fig. 1A), while the levels of the remaining factors, including Cdk4, were virtually indistinguishable from those obtained by serum stimulation. The behavioral difference between Cdk6 and Cdk4 was further noticeable in another experiment. When MC3T3-E1 cells were treated with FGF-2, a potent stimulator of osteoblast proliferation, the level of Cdk4, but not that of Cdk6, was markedly elevated (Fig. 1B).

To confirm that the blocked induction of Cdk6 was faithfully reflected by its kinase activities, we assayed the activities of Cdk6 and Cdk4 during serum stimulation in the presence and absence of BMP-2. When the cells were stimulated with serum, Cdk6 activity increased at 12 h and remained high at least until 48 h. In contrast, when the cells were stimulated with serum containing BMP-2, Cdk6 activity increased at 6 h, but rapidly decreased to the basal level by 12 and 24 h, the times expected for the commitment to differentiation to take place (Fig. 1C). These activities were roughly correlated with the amounts of immunoprecipitated Cdk6, which faithfully reflected its amounts in whole-cell lysates (Fig. 1A), except for the BMP-2-treated 6-h sample, from which Cdk6 was more efficiently immunoprecipitated. This result was reproducible, but its reason was unclear.

On the other hand, there was no significant difference in the time course and extent of Cdk4 activation between BMP-2-treated and untreated MC3T3-E1 cells. Thus, despite the fact that Cdk4 and Cdk6 are structurally homologous (11) and share D cyclins as their catalytic partners, only the expression of Cdk6 was significantly influenced by BMP-2 treatment. We did a similar experiment with proliferating MC3T3-E1 cells and observed a similar down-regulation of Cdk6 upon BMP-2 treatment, although it was less obvious, perhaps due to the lack of synchronization in their cell cycle progression (data not shown).

Cdk6 down-regulation is not specific to this cell line and is a more general phenomenon. We performed the same Western blot analysis with a culture of primary osteoblasts isolated from neonatal mouse calvariae and obtained the same results. Treatment with BMP-2 during serum stimulation completely blocked the induction of Cdk6 at 24 and 32 h, whereas Cdk4 and Cdk2 were uninfluenced (Fig. 1D). These results show that Cdk6 was specifically down-regulated during the commitment to BMP-2-induced osteoblast differentiation.

BMP-2-led Cdk6 down-regulation is exerted at the transcriptional level. We performed a semiquantitative RT-PCR analysis of the Cdk6 transcript and found that *cdk6* mRNA disappeared when MC3T3-E1 cells were stimulated with BMP-2 (Fig. 2A). In contrast, BMP-2 did not significantly influence the stability of either *cdk6* mRNA or protein. When the cells were stimulated with serum for 6 h and then treated with

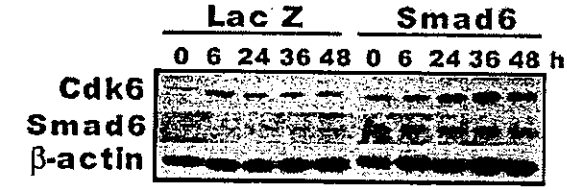

FIG. 3. Smad6 overexpression effectively blocks BMP-2-led down-regulation of Cdk6. MC3T3-E1 cells were infected with a recombinant adenovirus carrying the *smad6* or *lacZ* gene and were subsequently growth arrested by incubation in a low-serum-level medium for 48 h. The cells were then stimulated with serum in the presence or absence of BMP-2. The expression of Cdk6 and Smad6 was determined by Western blotting, with β-actin used as a loading control.

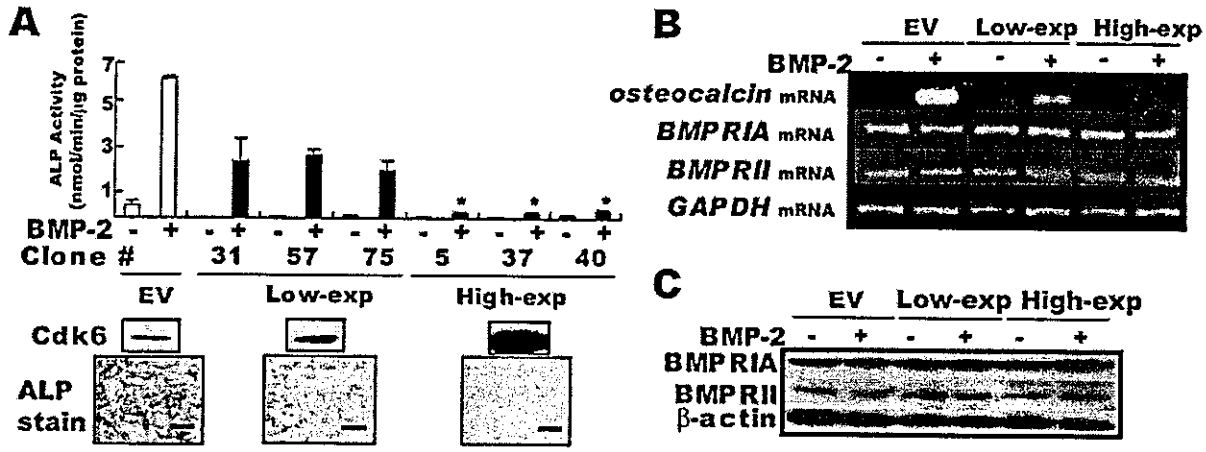

FIG. 4. Overexpression of Cdk6 inhibits BMP-2-induced osteoblast differentiation. MC3T3-E1 cell clones expressing low (no. 31, 57, and 75) or high (no. 5, 37, and 40) levels of Cdk6 and empty vector-transfected MC3T3-E1 (EV) cells were induced for osteoblast differentiation by treatment with BMP-2 according to the standard protocol. (A) After 72 h of treatment, the induced ALP activity was assayed (top). The middle panel shows Western blot data for Cdk6 in growing empty vector-transfected cells and cells from clones 31 and 40. *, $P < 0.1$; there is a significant difference from the ALP activity of BMP-2-treated empty vector-transfected cells. The bottom panels show ALP staining of empty vector-transfected cells and clones 31 and 40. Bars, 100 μm. (B) Levels of osteocalcin, BMPRIA, and BMPRII mRNAs, as determined by semiquantitative RT-PCRs with empty vector-transfected cells and clones 31 and 40 stimulated for 48 h with or without BMP-2. GAPDH mRNA was used as a control for the RNA preparations. (C) Protein levels of BMPRIA and BMPRII in empty vector-transfected cells and clones 31 and 40 stimulated for 48 h with or without BMP-2.

actinomycin D in the presence or absence of BMP-2, there was no difference in the rate of disappearance of the Cdk6 transcript between the treatment and nontreatment groups (Fig. 2B).

Cdk4 is known to be degraded by the ubiquitin-proteasome system (27). Because Cdk6 and Cdk4 are siblings and execute similar functions, we assumed that Cdk6 was likely to be degraded by the same proteolytic system. When MC3T3-E1 cells were treated with MG132, a potent inhibitor of this proteolytic system, during serum stimulation in the absence of BMP-2, the level of Cdk6 was elevated two- to threefold, consistent with this assumption (Fig. 2C). In the presence of BMP-2, MG132 treatment elevated the level of Cdk6 by the same degree, suggesting that there is no acceleration of Cdk6 degradation by treatment with this differentiation inducer. To further confirm that BMP-2 did not affect the stability of the Cdk6 protein, we constructed and analyzed MC3T3-E1 cell clones that constitutively expressed Cdk6 at low and high levels. BMP-2 treatment did not influence the levels of Cdk6 protein expressed from the constitutive EF1α promoter (Fig. 2D). These findings indicate that BMP-2 down-regulates Cdk6 expression mainly, if not exclusively, by transcriptional repression.

Smads mediate BMP-2-induced down-regulation of Cdk6. A differentiation signal invoked by BMP-2 is known to be mediated by Smad proteins, particularly R-Smads and Co-Smads, while I-Smads, such as Smad6 and Smad7, inhibit this signaling (6). To investigate whether Smads mediate Cdk6 down-regulation, we overexpressed Smad6 in MC3T3-E1 cells by use of an adenovirus vector and examined its effect on BMP-2-led Cdk6 down-regulation. As shown in Fig. 3, BMP-2-led Cdk6 down-regulation was completely abolished by the overexpression of Smad6, indicating that Smads do indeed mediate the BMP-2-led Cdk6 down-regulation.

Osteoblasts overexpressing Cdk6 strongly resist BMP-2-invoked differentiation. As discussed above, Cdk6 was down-regulated during BMP-2-invoked osteoblast differentiation. Consequently, a key question is whether this down-regulation is essential for osteoblast differentiation or not. To address this question, we constructed >100 MC3T3-E1 cell clones that stably expressed various levels of Cdk6 by transfecting MC3T3-E1 cells with an expression vector harboring *Cdk6* cDNAs and then tested their ability to respond to BMP-2 and to differentiate into mature osteoblasts. Figure 2D shows the protein levels of Cdk6, Cdk4, and Cdk2 in some representative clones that were treated with BMP-2 or were left untreated compared to the protein levels in similarly treated empty vector-transfected control MC3T3-E1 cells. The Cdk4 and Cdk2 protein levels were not affected by the overexpression of Cdk6, suggesting the absence of any particular compensatory regulation of Cdk4 or Cdk2 expression upon Cdk6 overexpression.

The ability of BMP-2 to induce osteoblast differentiation, as monitored by ALP production and osteocalcin expression, which are well-characterized early and late differentiation markers, respectively, was then studied with control cells and low (~2-fold) and high (>10-fold) Cdk6 expressers. The induction of ALP upon BMP-2 treatment was inhibited significantly in the low expressers and completely in the high expressers (Fig. 4A). Osteocalcin mRNA, as measured by semiquantitative RT-PCR, was markedly reduced in the low expressers and was undetectable in the high expressers (Fig. 4B). Thus, a twofold overexpression of Cdk6, or the same level of exogenous Cdk6 expression as endogenous expression, already showed a strong inhibitory effect on differentiation. This implies that the presence of the original level of Cdk6 expression was enough to markedly inhibit the BMP-2-invoked differentiation of MC3T3-E1 cells.

TABLE 1. Proliferation and cell cycle distribution of MC3T3-E1 cells that overexpress Cdk6[a]

Cell type	BrdU incorporation (OD) at indicated time (h) in presence or absence of BMP-2				Flow cytometric analysis result in presence or absence of BMP-2			
	24		72		% G_0/G_1		%G_2/M	
	−	+	−	+	−	+	−	+
Empty vector	0.37 ± 0.01	0.37 ± 0.12	0.07 ± 0.01	0.08 ± 0.01	78 ± 0	80 ± 1	16 ± 1	15 ± 0
Low expresser	0.41 ± 0.05	0.37 ± 0.08	0.06 ± 0.02	0.08 ± 0.02	78 ± 1	76 ± 0	17 ± 1	18 ± 1
High expresser	0.55 ± 0.07	0.43 ± 0.07	0.05 ± 0.01	0.06 ± 0.01	77 ± 0	79 ± 1	15 ± 1	15 ± 1

[a] Cell proliferation was determined by BrdU incorporation after 24 and 72 h of culture in the presence and absence of BMP-2. Cell cycle distribution was determined by flow cytometric analysis of cells after 24 h of culture. Three representative clones (31, 57, and 75 and 5, 37, and 40, respectively) were chosen from the low- and high-expressing group. Data are expressed as means ± standard deviations after analysis of cells in eight separate wells for each clone.

The Cdk6-led resistance to osteoblast differentiation is unlikely to be caused by an unexpected interference of the BMP-2/Smads signaling pathway by the overexpressed Cdk6. Neither the mRNA nor the protein levels of the BMP receptors BMPRIA and BMPRII were significantly affected by Cdk6 expression (Fig. 4B and C).

Overexpression of Cdk6 does not influence proliferation of osteoblasts. Because Cdk6 promotes the G_1-S transition, the suppression of osteoblast differentiation by overexpressed Cdk6 could be a mere consequence of its execution of this role. We therefore examined the effects of both BMP-2 and Cdk6 overexpression on the G_1-S transition and the proliferation of MC3T3-E1 cells. Empty vector-transfected MC3T3-E1 cells, as well as the low and high Cdk6 expressers, were similarly arrested in quiescence, stimulated with serum in the presence or absence of BMP-2, and analyzed for S-phase entry as well as for cell populations in G_0-G_1 and G_2-M by BrdU incorporation and flow cytometric analyses (Table 1). Cell proliferation was also monitored in the presence and absence of BMP-2 by an XTT assay (Fig. 5). The overexpression of Cdk6 did not cause any significant changes in either the cell cycle distribution or the proliferation rate of the cells, regardless of whether the cells were stimulated with BMP-2 or not. These results suggest that the inhibitory effect of Cdk6 on osteoblast differentiation is not exerted via cell cycle regulation.

The Cdk6-exerted differentiation block is correlated with a loss of the binding of Runx2/Cbfa1, but not Rb, to the osteocalcin promoter. Rb, a potent repressor of the E2F-DP transcriptional factor that is essential for the onset of S phase, has been reported to also act as a transcriptional coactivator for Runx2/Cbfa1, a key transcriptional factor for osteoblast differentiation (23). Since Rb is a direct target of Cdk6 for cell cycle control, we examined whether Rb mediates the Cdk6-exerted inhibition of osteoblastic differentiation by determining the effects of overexpressed Cdk6 on the vivo binding of Runx2/Cbfa1 and Rb to the osteocalcin promoter during BMP-2 treatment. To this end, we performed a ChIP assay. The specificities of the anti-Runx2/Cbfa1 and anti-Rb antibodies used for this assay were confirmed by the lack of precipitation of the irrelevant myogenin promoter, but the clear precipitation of the osteocalcin promoter, by both antibodies (Fig. 6).

Using these antibodies, we compared the binding levels of Runx2/Cbfa1 and Rb to the osteocalcin promoter in empty vector-transfected MC3T3-E1 cells and in low and high Cdk6 expressers at day 1 (a time just after the differentiation commitment) and day 4 (well after the onset of full differentiation phenotypes for MC3T3-E1 cells) post-BMP-2 treatment. As shown in Fig. 6A, on day 1 Runx2/Cbfa1 bound slightly to the osteocalcin promoter in the empty vector-transfected MC3T3-E1 cells, but not in either the low or high Cdk6 expressers, whereas no binding of Rb to this promoter was detected in any of these cells. On day 4, when osteocalcin was fully expressed, the binding of Runx2/Cbfa1 to this promoter was clearly detected in the empty vector-transfected MC3T3-E1 cells and the low Cdk6 expresser, but not in the high Cdk6 expresser, in which osteoblast differentiation was completely blocked (Fig. 4) despite a high level of Runx2/Cbfa1 expression (Fig. 6B). Thus, there was a close correlation between osteoblast differentiation and the binding of Runx2/Cbfa1 to the osteocalcin promoter in Cdk6-led differentiation inhibition. In

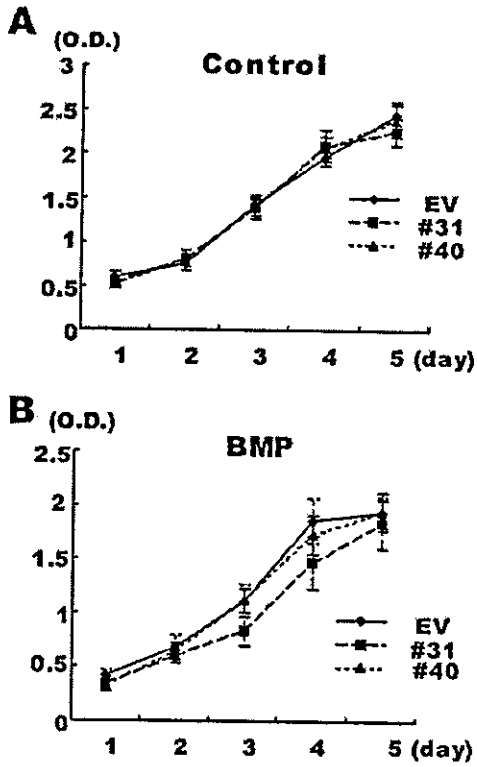

FIG. 5. Overexpression of Cdk6 does not influence proliferation of MC3T3-E1 cells. Proliferation rates were determined by XTT staining of empty vector-transfected cells (EV) and clones 31 and 40 cultured in the presence (B) or absence (A) of BMP-2, with cell sampling done every day.

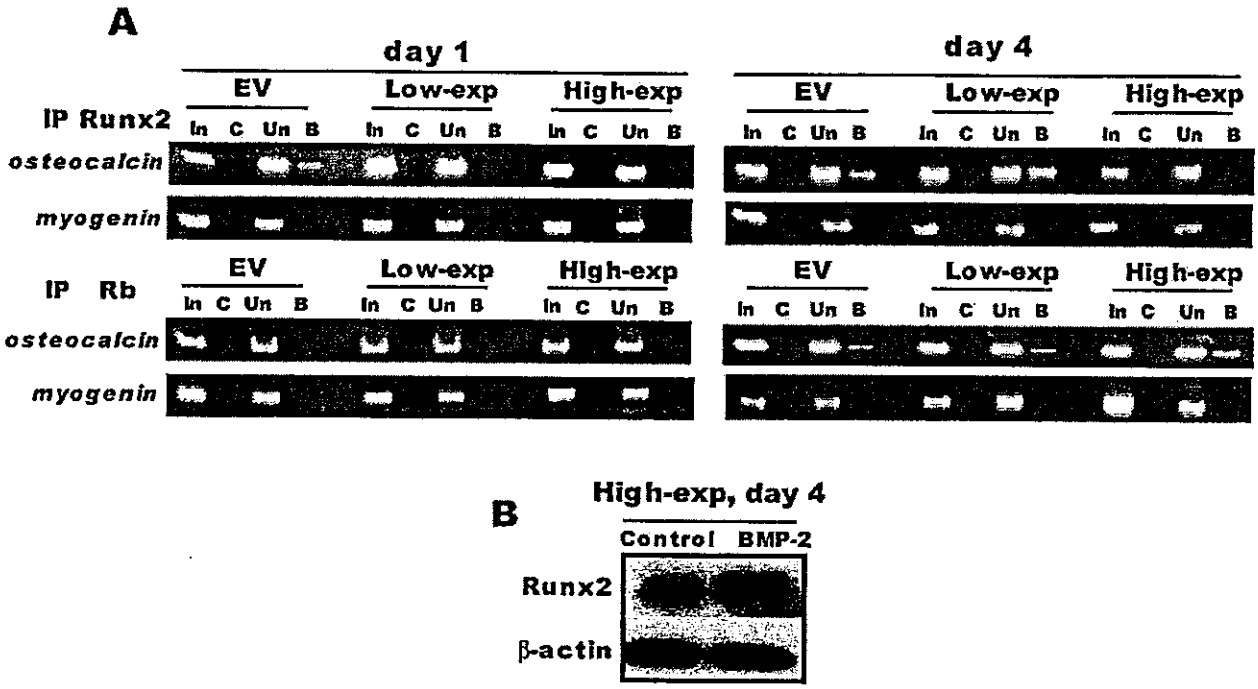

FIG. 6. Cdk6-exerted differentiation block is correlated with a loss of binding of Runx2/Cbfa1, but not Rb, to the osteocalcin promoter. (A) ChIP assay performed with empty vector-transfected MC3T3-E1 cells (EV) and clones 31 (low Cdk6 expresser) and 40 (high Cdk6 expresser) cultured for 1 and 4 days with BMP-2, as described in Materials and Methods. IP Rb, immunoprecipitation with an anti-Rb antibody; IP Runx2, immunoprecipitation with an anti-Runx2/Cbfa1 antibody; In, total DNA input for each sample; C, immunoprecipitation with control serum; Un, PCR from the supernatant after immunoprecipitation; B, PCR from immunoprecipitation product. The primer sets for PCRs of the osteocalcin and myogenin promoter regions are described in Materials and Methods. (B) Runx2/Cbfa1 is expressed in a high Cdk6 expresser cultured for 4 days with or without BMP-2. The level of Runx2/Cbfa1 was determined by Western blotting. The loading control is β-actin.

contrast, there was no apparent correlation between Rb binding and osteoblastic differentiation. On day 4, the binding of Rb to the osteocalcin promoter was detected, as reported previously (23), but it was present in all of the cells, despite the fact that osteoblastic differentiation in the high Cdk6 expresser was completely blocked. Moreover, Rb seemed to bind the promoter independently of Runx2/Cbfa1, because in the high Cdk6 expresser, Rb bound the promoter without the binding of Runx2/Cbfa1.

These ChIP assay results indicate that Rb is unlikely to mediate the Cdk6-led differentiation inhibition, although it is certainly required for the efficient osteoblast differentiation of MC3T3-E1 cells (23). In addition, the loss of Runx2/Cbfa1 binding to the osteocalcin promoter during Cdk6-exerted differentiation inhibition raises the possibility that Cdk6 may inhibit osteoblastic differentiation by blocking the promoter-binding ability of the Runx2/Cbfa1 transcriptional factor.

DISCUSSION

In the present study, we have shown that Cdk6 expression is shut down mainly at transcription upon BMP-2 treatment and that this shutdown, mediated by BMP-2-activated Smad signaling, is required for efficient osteoblast differentiation. Osteoblastic cells, including the presently used MC3T3-E1 cell line and primary mouse osteoblasts, express both Cdk4 and Cdk6, yet only Cdk6 is critically involved in the commitment to dif-

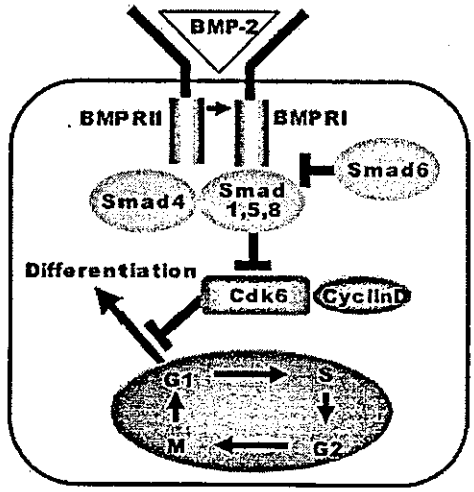

FIG. 7. Schematic presentation of the mechanism by which Cdk6 inhibits osteoblastic differentiation. BMP-2 binds the type II receptor, which subsequently activates the type I receptor by direct association. The activated type I receptor directly phosphorylates R-Smads (Smads 1, 5, and 8) and promotes their complex formation with Co-Smad (Smad4). The R-Smads/Co-Smad complexes are then translocated into the nucleus, where they repress the transcription of the *cdk6* gene and permit osteoblastic differentiation to take place.